

Article

GIS-Based RUSLE Reservoir Sedimentation Estimates: Temporally Variable C-Factors, Sediment Delivery Ratio, and Adjustment for Stream Channel and Bank Sediment Sources

Patrick J. Starks *, Daniel N. Moriasi and Ann-Marie Fortuna 

Agroclimate and Hydraulic Engineering Research Unit, United States Department of Agriculture, Agricultural Research Service, Oklahoma and Central Plains Agricultural Research Center, 7207 W. Cheyenne St., El Reno, OK 73036, USA; daniel.moriasi@usda.gov (D.N.M.); ann-marie.fortuna@usda.gov (A.-M.F.)

* Correspondence: patrick.starks@usda.gov

Abstract: The empirical Revised Universal Soil Loss Equation (RUSLE) has been adapted to geographical information system (GIS) frameworks to study the spatial variability of soil erosion across landscapes and has also been used to estimate reservoir sedimentation. The literature presents contradictory results about the efficacy of using RUSLE in a GIS context for quantifying reservoir sedimentation, requiring further evaluation and validation of its estimates relative to measured reservoir sedimentation. Our primary objective was to determine if these contradictory results may be a function of the RUSLE's inability to account for sediments derived from gullies, stream channels, or stream banks; the temporal variability of some of RUSLE's empirically based factors such as the land cover/land management (C-) factor; and in some model renditions, the choice of value for the sediment delivery ratio (SDR). The usefulness of adjusting these estimates using a regional representative value of gully/stream bank sediment contributions was also assessed. High-spatial horizontal resolution (2 m) digital elevation models (DEMs) for 12 watersheds were used together with C-factor data for five representative years in a GIS-based RUSLE model that incorporates SDR within a sediment routing routine to study the impacts of choice of C-factor and SDR on reservoir sedimentation estimates. Choice of image date for developing C-factors was found to impact reservoir estimates. We also found that the value of SDR for some of the study watersheds would have to be unrealistically small to produce sedimentation estimates comparable to measured values. Estimates of reservoir sedimentation were comparable to measured data for 5 of the 12 watersheds, when the regionally based adjustment for gully/stream bank contributions was applied. However, differences remained large for the remaining seven watersheds. Statistical analysis revealed that certain combinations of geomorphic, pedologic, or topographic variables could be used to predict the degree of sediment underestimation with a significant and high level of correlation ($0.72 < R^2 \leq 0.99$; p -value < 0.05). Our findings indicate that the level of agreement between GIS-based RUSLE estimates of reservoir sedimentation and measured values is a function of watershed characteristics; for example, the area-weighted soil erodibility (K-) factor of the soils within the watershed and stream channels, the stream entrenchment ratio and bank full depth, the percentage of the stream corridor having slopes $\geq 21^\circ$, and the width of the stream flood way as a percentage of the watershed area. Within the context of GIS, these metrics are easily obtained from digital elevation models and publicly available soils data and may be useful in prioritizing reservoirs' assessments for function and safety.



Citation: Starks, P.J.; Moriasi, D.N.; Fortuna, A.-M. GIS-Based RUSLE Reservoir Sedimentation Estimates: Temporally Variable C-Factors, Sediment Delivery Ratio, and Adjustment for Stream Channel and Bank Sediment Sources. *Land* **2023**, *12*, 1913. <https://doi.org/10.3390/land12101913>

Academic Editor: Vincent Chaplot

Received: 22 August 2023

Revised: 22 September 2023

Accepted: 3 October 2023

Published: 12 October 2023



Copyright: © 2023 by the authors. Licensee MDPI, Basel, Switzerland. This article is an open access article distributed under the terms and conditions of the Creative Commons Attribution (CC BY) license (<https://creativecommons.org/licenses/by/4.0/>).

Keywords: geographical information system (GIS); erosion; channel instability; sediment delivery ratio (SDR)

1. Introduction

During the 1930s, severe drought and poor conservation practices in Oklahoma and the Southern Great Plains resulted in decreased vegetative cover, which combined with

subsequent periods of intense rainfall caused increased erosion and flooding [1]. Because of these natural disasters, the U.S. Congress passed the Flood Control Act of 1944 (PL-534) and the Watershed Protection and Flood Prevention Act of 1954 (PL-566) to minimize soil erosion and to prevent flooding [2,3]. As a result of these Acts, the Washita River Basin (WRB) in Oklahoma was 1 of 11 pilot watershed projects selected for the construction of flood control reservoirs. Through the PL-534 and PL-566 projects, the United States Department of Agriculture (USDA) Natural Resources Conservation Service in Oklahoma provided technical and financial assistance for the construction of 2107 flood control dams (~20% of the national total) [1]. Forty-five of these dams were built in the Little Washita River Watershed (LWREW, located in the WRB) between 1969 and 1982 [4].

Bennett et al. [5] projected that by 2020 about 50% of the USDA Natural Resources Conservation Service (NRCS) reservoirs would be near the end of their projected 50-year service life due to sedimentation. Reduction in reservoir sediment trapping can lead to reduced usable pool depth and flood storage capacity and decreased future sediment storage, projected lifespan, and agricultural productivity [6]. For these reasons, these reservoirs need to be evaluated for rehabilitation or decommissioning [7].

Due to aging of these NRCS structures, Section 313 of Public Law 106–472 [8] provided authorization to conduct an evaluation of the reservoirs for possible extension of service life of the structures, for conformance to applicable safety and performance standards, or for decommissioning. A common first step in the assessment for rehabilitation is to survey the amount of sediment in the reservoir [6]. Often, such assessments require labor intensive and costly measures to conduct, for example, acoustic profiling and sediment coring, which would become more prohibitive if trying to assess sedimentation for many reservoirs. Modeling is a good choice for conducting preliminary assessments, especially in the context of prioritizing watersheds for follow-up investigations. However, process-based models such as Water Erosion Prediction Project (WEPP) [9] and European Soil Erosion Model (EUROSEM) [10] often require data that may not be available or are difficult to acquire [11]; thus, empirical models such as the Revised Universal Soil Loss Equation (RUSLE) [12] are often used. RUSLE is an improvement upon its USLE predecessor [13], an empirical equation developed from >10,000 plot-years of soil erosion and runoff data [13] and originally intended for field-based applications. The RUSLE requires five inputs to calculate soil loss: a rainfall and runoff factor (R), a soil erodibility factor (K), a slope length and steepness factor (LS), a land cover and management factor (C), and a support practice factor (P). Due to increased computing power over the last several decades and the development of geographical information systems (GIS), RUSLE has been increasingly used for spatial analysis of soil erosion for landscapes and watersheds of various sizes [14–16].

The review of the literature indicates that many GIS-based RUSLE soil erosion studies focused on temporal erosion trends and the assessment of relative changes in sediment production [17] and for targeting erosion “hot spots” within watersheds [18]. There are a limited number of RUSLE-based studies that have been conducted wherein the spatial distribution of plant, soil, land management, rainfall, and topographic variables were used to estimate reservoir sedimentation for comparison against measured reservoir sediment accumulation [19–22]. However, the literature presents contradictory results for the efficacy of using RUSLE in a GIS context for quantifying reservoir sedimentation. Boomer et al. [19] applied the USLE and RUSLE2 (second generation of RUSLE) to 78 small sub-watersheds within the Chesapeake Bay watershed and reported that the USLE family of models exceeded measured annual average sediment delivery by more than 100%. Moges et al. [20] reported that GIS-based RUSLE estimates were ~1.3, and 1.7 times larger than those measured for the Selamko and Shina watersheds, respectively, in the Ethiopian Blue Nile basin. Kaffas et al. [12] also used a spatially distributed version of RUSLE to estimate reservoir sedimentation for the Rio di Pusteria reservoir in the Italian Alps. In that study, the researchers used two different methods to calculate the RUSLE R-factor, i.e., one representing the 5 yr study period, and the second representing the long-term average conditions. Kaffas et al. [21] also adjusted the initial RUSLE estimates via a sediment

delivery ratio (SDR) and found that estimated reservoir sedimentation was within 3.1% and –23.2%, depending upon R-factor method used, and was within 12.5% of the measured value if the SDR adjustment was used. Bufalini et al. [22] compared bathymetric sediment measurements of a reservoir in central Italy, and estimated via a GIS-based RUSLE. In their study, Bufalini et al. [22] calculated the P-factor in three separate ways, which had a profound effect on the RUSLE sediment estimates. These researchers concluded that a GIS-based RUSLE approach could be used to reasonably estimate reservoir sedimentation if the RUSLE parameters were properly calibrated.

Multiple authors have noted that the main weakness of the RUSLE model is that it does not account for gully erosion, stream bank instabilities, and channel contributions to the sediment load [15,19–21,23–25]. Simon and Rinaldi [26] showed that stream bank erosion accounted for 64 to 90% of the total sediment load for four streams in the Southeastern U.S. Wilson et al. [27] showed, using ratios of ^7Be to ^{210}Pb , that eroded surface soils in the Fort Cobb Reservoir watershed (located in Southwestern Oklahoma) only accounted for 46% of suspended sediments in streams following a runoff event. Simon and Klimetz [28] noted that ~60% of the stream channels in the LWREW—our study area—are unstable and contribute a considerable amount of sediment to downstream reservoirs. Other weaknesses of the RUSLE approach were outlined by Benavidez et al. [29] and included choice of spatial resolution of the digital elevation models (DEMs) used in the study (which affects the calculation of the LS factor), granularity and scale of land cover characteristics, and choice of values for the RUSLE factors. These authors added that another limitation of the RUSLE approach is the lack of validation data to verify the model's output. Therefore, there is a need for further evaluation and validation of the GIS-based RUSLE approach to estimate reservoir sedimentation, specifically regarding the impact of temporally variable land cover data sets and the impact of channel and stream bank contributions to reservoir sedimentation. It may be possible to improve the usefulness of a GIS-based RUSLE approach through evaluation of linkages between measured reservoir sedimentation and easily obtainable geomorphic, pedologic, and topographic metrics.

Our objectives are as follows: (1) quantify the impact of temporally variable C-factors on the estimation of long-term average reservoir sedimentation, (2) determine if a regionally based adjustment, suggested by the results of Wilson et al. [27], can be used as a first-order correction to account for sediment contributions from gullies, stream channels, and stream banks, and (3) examine linkages between estimated reservoir sedimentation and watershed, stream, stream corridor, and stream bank variables acquired from high-spatial horizontal resolution (2 m) digital elevation models (DEMs), satellite-based land cover data sets, and publicly available soils data.

2. Material and Methods

2.1. Study Sites

2.1.1. General Description

The study was conducted on 12 watersheds and their accompanying reservoirs located in the LWREW, in Southwestern Oklahoma, USA [1] (Figure 1). The LWREW is ~610 km² in size and is characterized by gently to moderately rolling topography with a maximum relief of 490 m [4]. The soils in the central section of the LWREW are sandy in texture, whereas silty loam and loamy soils are found in the western and eastern sections. The 1991–2020 normal annual precipitation was ~807 mm, with about 27 and 20% of the annual total precipitation occurring in the months of May–June and September–October, respectively. The annual average daily temperature is 15.6 °C, with annual maximum and minimum air temperatures occurring in July (27.9 °C) and January (3.2 °C), respectively [30].

The reservoirs evaluated in this study were impounded between 1969 and 1982 (Table 1) and are further described by Moriasi et al. [1]. The watershed drainage areas, reservoir surface areas, and principal land uses [4] are provided in Table 1. The dominant land cover within each watershed is grassland, which varies between watersheds, ranging from 44 to 80%. In four of the twelve watersheds, 21 to 44% of their areas are tree/shrub

lands, and in another four, 15 to 43% of their areas are cropped areas. These subdominant land cover categories (Table 1) were used in the statistical analysis to identify possible differences in reservoir sedimentation due to land cover factors.

Moriassi et al. [1] conducted a bathymetric survey of the twelve reservoirs during 14–25 May 2012 using a multifrequency acoustic profiling system. The details of this survey and the device used to collect the data are provided by Moriassi et al. [1]. The impoundment period (representing the time from impoundment to the survey date) varied from 29.6 yr (Reservoir 20) to 42.6 yr (Reservoir 42) (Table 1). The measured reservoir sediment volumes ranged from 24,155 to 439,581 m³ (Table 1).

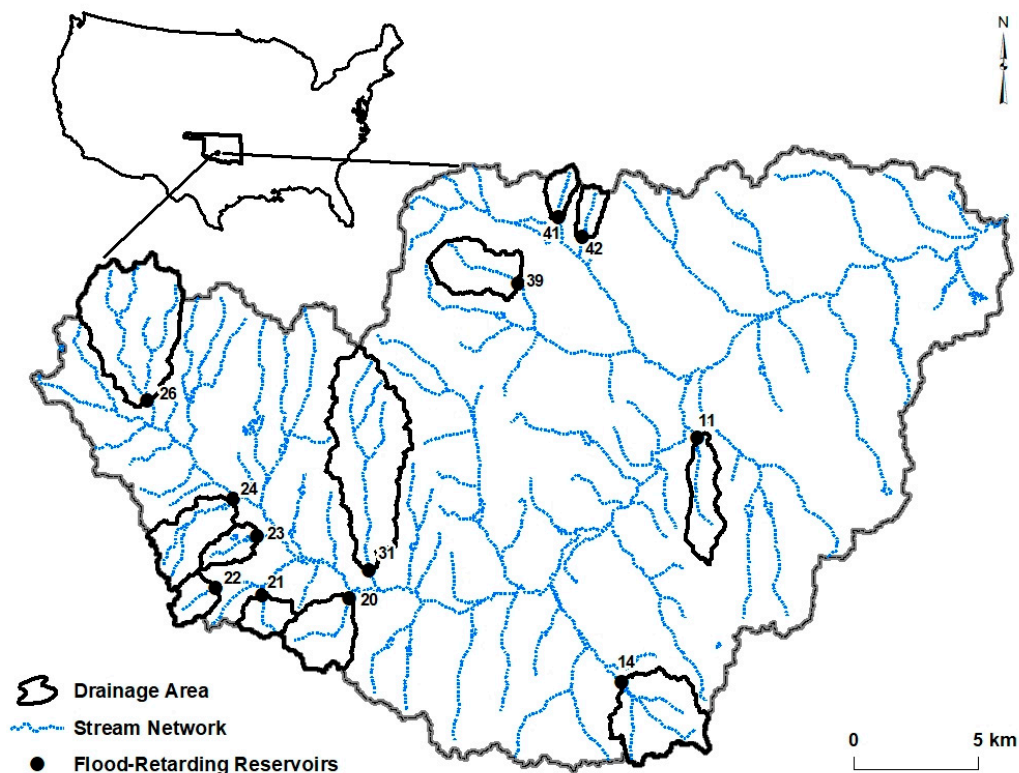


Figure 1. Location and identification numbers of the study watersheds within the LWREW.

2.1.2. Watershed and Stream Geomorphic and Topographic Variables

In addition to the data required to run the RUSLE model, several variables were identified or developed (Figure 2) and measured to assist in interpreting differences between measured and estimated reservoir sedimentation. These variables include percentage of watershed area having slopes $\geq 21^\circ$ ($\%W_{\text{slope} \geq 21}$), watershed basin relief (W_{rlf}), watershed valley length (W_{vl}), stream slope (S_{slope}), stream thalweg length (S_{thal}), and stream sinuosity (S_{sn}).

Watershed slope images were created within the Idrisi TerrSet 2020 (Clarke Labs, Clarke University, Clarke, MA, USA) GIS software, and the pixel-based values were downloaded for statistical evaluation. The $\%W_{\text{slope} \geq 21}$ was developed based on the findings of [1], which indicated that the land area with slopes $\geq 21^\circ$ was a useful metric to quantify topographic effects on reservoir sedimentation. Slope images for each watershed are shown in Supplemental Figures S1–S12. Basin relief was calculated as the difference between the highest and lowest (outlet) elevations in the watershed. Stream thalwegs were digitized from each watershed's digital elevation model (DEM), and their lengths were recorded. Watershed valley length was determined as the straight-line distance running parallel with the stream from the top to the watershed outlet. Stream sinuosity was determined as the ratio of $S_{\text{thal}}:W_{\text{vl}}$. Interpretation of the sinuosity values is provided in Supplemental Table S1. At the watershed scale, the pedologic information consists of

that required by the RUSLE model, namely, the spatially distributed K-factors (described below and shown in Supplemental Figures S1–S12). The K-factor data was also used to calculate a single area-weighted K-factor (WK) for each watershed and to quantify the percentage of each watershed area having low, medium, and high K-factor soils (WLK, WMK, and WHK).

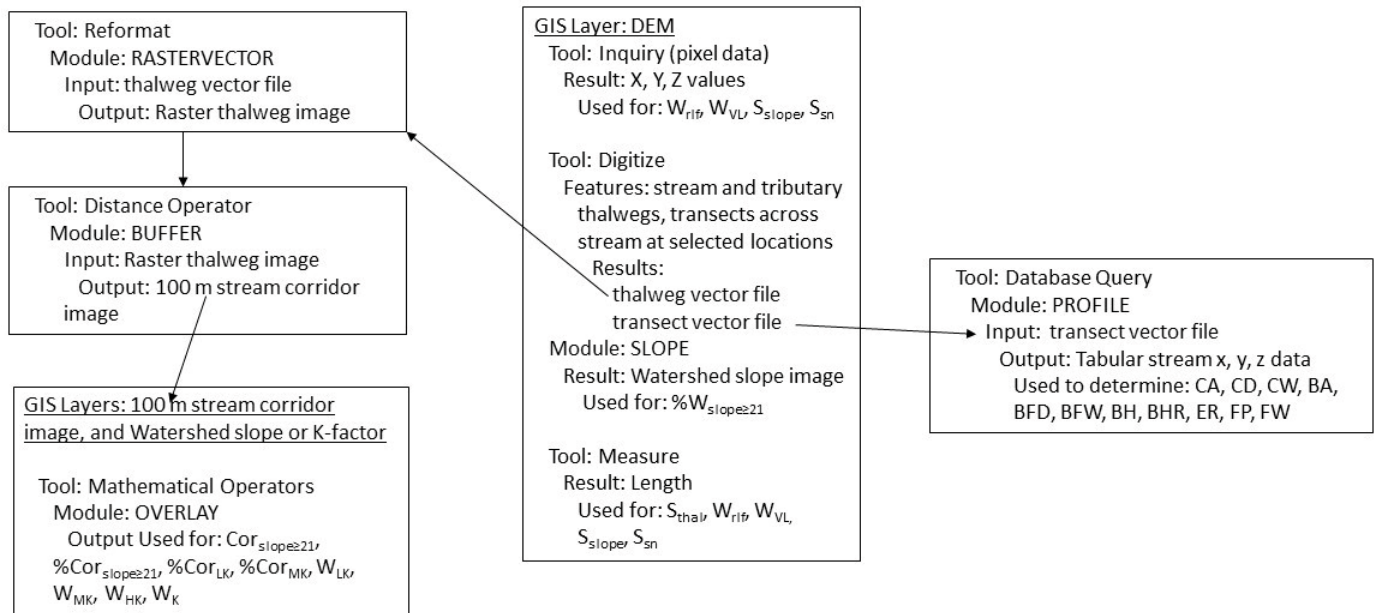


Figure 2. Methodology used to develop watershed, stream, stream corridor, and within-channel variables from digital elevation models (DEMs) and K-factor images from each watershed.

2.1.3. Stream Corridor Variables

Using TerrSet, each watershed's DEM was displayed on a monitor from which the thalweg of the main stream and its visible (on the DEM) tributaries were manually digitized. From the resulting thalweg images, a 100 m corridor (50 m either side of the thalwegs) was generated using the BUFFER module. The stream corridor images were then used to extract and quantify the actual corridor area and percentage of the corridor area having slopes $\geq 21^\circ$ ($Cor_{slope \geq 21}$ (m^2) and $\%Cor_{slope \geq 21}$, respectively). The density of $Cor_{slope \geq 21}$ was quantified as a ratio compared to W_{vl} ($Cor_{slope \geq 21} : W_{vl}$ ($m^2 m^{-1}$)). Visual inspection of the watershed slope maps indicated that many streams had substantial areas within their corridors having high slope values; thus, these three variables may act as proxies for contributions of sediment from gullies and unstable stream banks. The stream corridor images were also used to determine the percentage of corridor area having low, moderate, or high K-factor soils ($\%Cor_{LK}$, $\%Cor_{MK}$, and $\%Cor_{HK}$).

Table 1. Watershed/reservoir identification number (ID), reservoir construction completion date, watershed area draining into the reservoir (W_A), percentage of major land uses with each watershed, the subdominant land use group to which each watershed was assigned, bathymetric survey date, reservoir impoundment period from time of completed construction to the bathymetric survey date, and measured sediment volume from completion date of reservoir construction to date of the bathymetric survey. Data obtained from Moriasi et al. [1] and Allen and Naney [4].

Watershed/ Reservoir ID	* Date Construction Completed (dd/mm/yr)	W_A (km ²)	% Watershed Area under Land Cover Type			Subdominant Land Cover ID	Bathymetric Information		
			Crop	Grass	Tree/Shrub		Survey Date	Impoundment Period (yr)	Sediment Volume (m ³)
11	6 November 1973	4.9	10	73	15	Grass	24/05/2012	39.0	36,991
14	14 April 1978	10.8	5	75	16	Grass	15/05/2012	34.1	146,856
20	27 October 1982	6.7	2	60	33	Tree/Shrub	22/05/2012	29.6	115,906
21	DD May 1970	2.8	3	80	11	Grass	22/05/2012	42.1	37,485
22	8 April 1977	2.9	15	69	13	Grass	18/05/2012	35.1	96,917
23	27 July 1971	2.5	34	59	2	Crop	17/05/2012	40.8	24,155
24	8 November 1976	7.0	43	46	6	Crop	17/05/2012	35.5	72,256
26	DD December 1971	18.0	42	50	2	Crop	16/05/2012	40.4	439,581
31	14 September 1978	19.2	14	60	21	Crop	23/05/2012	33.7	308,015
39	26 June 1978	6.3	1	56	35	Tree/Shrub	24/05/2012	33.9	69,174
41	DD October 1969	2.0	2	44	44	Tree/Shrub	14/05/2012	42.5	36,868
42	DD October 1969	1.9	4	66	24	Tree/Shrub	25/05/2012	42.6	27,867

* DD indicates that the day of year was not reported.

2.1.4. Within-Channel Variables

The watershed slope images were used to visually identify sections of each stream channel that were similar in terms of their general bank steepness. Using the GIS software, one or more transects were drawn perpendicular to the thalweg of the main stream and of sufficient length to include the stream's banks and floodplains. From these transects, stream channel geomorphic variables were measured and included channel cross-sectional area (CA), channel depth (CD), and channel width (CW). For V- and rectangular-shaped cross-sections, CA was based on CD and CW and computed as the area of either a triangle or a rectangle. For more complicated shapes, the cross-section was gridded from which the area was determined from the number of grid elements of known area. The ratio CW:CD was also calculated, which is related to the physical processes governing the distribution of energy and resultant sediment transport. Other within-channel (IC) geomorphic variables were selected from [31]'s stream classification metrics, as described by USDA NRCS [32], and from metrics used in the Bank Stability and Toe Erosion model (BSTEM) [33]. Metrics from Rogsen [31] include the bank full depth (BFD), bank full width (BFW), BFW:BFD, and entrenchment ratio (ER). The BFD is the depth at which the most effective movement of sediments occurs (typically streamflow at a 1.5 yr return interval) and is determined from the bank full discharge in gaged streams. The BFD is the most critical variable that needs to be determined correctly as it is used to calculate the BFW and ER. In ungaged streams, regional curves that relate watershed area to BFD can be used if the regional curve is representative of local conditions. If the BFD cannot be determined either from stream gage data or from an appropriate regional curve, it should be determined directly in the field and may be based on the presence of point bars, aggraded material in the channel, changes in bank slope, or indications of bank scour. However, such field investigations were not practical for this study. Therefore, we used surrogate indicators for the "apparent" BFD that included the presence of aggraded sediments in the streambed, changes in bank slope, or scour marks (undercuts in the bank) as visually detected in the stream cross-section profiles derived from the 2 m DEMs. The ER is defined as the ratio of the flood-prone width (the width of the channel at 2xBFD) to the BFW and is a measure of the "connectedness" between the stream channel and its floodplain (FP). Entrenched streams are not well connected to their FPs; thus, sediments derived from stream banks and channels are more quickly and efficiently moved directly to the receiving reservoirs. Less entrenched streams have a higher likelihood of overtopping their banks where sediments derived from all sources may be deposited on the FP, thereby increasing their residence time within the watershed

before ultimately being deposited in the reservoir. The selected BSTEM variables include the bank angle (BA) and bank height (BH), which were also determined from the channel cross-sectional measurements. The BA was determined as the angle from a line parallel with the BFD elevation to the top of the bank. The BH was determined by the difference in elevation between the BFD and the top of the bank. Bank height ratio (BHR), a measure of channel incision [34], was determined as BH/BFD , where the BH value of the lowest of the two banks was used. Interpretation of numerical values of BA, BH, BHR, and ER are provided in Supplemental Tables S2–S4. We also determined the stream floodway area (FWA) as a percentage of the W_A from $FWA_{\%}W_A = CW \times S_{thal}/W_A \times 100$, which may be considered another measure of the connectedness between the stream channel and its FP. If two or more transects were acquired for a given stream segment, then the average of the respective variables within that segment was calculated. Variables in each segment were then weighted by the length of that segment relative to the sum of the lengths of all stream segments. The sum of the respective weighted individual variables was then used to represent the entire stream length.

Within-channel (IC) soil variables included the area-weighted percent sand and silt (IC_{Sa} and IC_{Si} , respectively) fractions, plasticity index (IC_{PI}), the percent of stream length with low, medium, and high K-factor soils ($\%IC_{LK}$, $\%IC_{MK}$, and $\%IC_{HK}$, respectively), and an area-weighted K-factor (IC_K). The IC_{PI} , a measure of soil erodibility, is the water content needed to change the soil from a semi-solid state (which is resistant to flow) to a liquid state where the soil moves freely. These soil-related variables were obtained from the USDA-NRCS Web Soil Survey [35] and were directly acquired from the website's data inquiry tools by manually digitizing a polygon surrounding the stream which was drawn as closely as possible to the top of the stream banks. The value of the above variables within the resultant soil mapping units and the percentage surface area of a given mapping unit within the polygon was then retrieved as tabular data from which area-weighted values of the variables were calculated.

2.2. GIS-Based RUSLE/SEDIMENTATION

2.2.1. RUSLE Model Description

The RUSLE is written as follows:

$$A = R \times K \times LS \times C \times P \quad (1)$$

where A is the calculated soil loss per unit area in units for K (metric ton \times ha \times hr)/(ha \times MJ \times mm). The R -factor accounts for the effects of raindrop impact and the amount and rate of runoff likely to be associated with rain [12]. The K and LS factors are developed with reference to a soil loss rate determined from a unit plot 22.13 m in length, continuously in clean-tilled fallow conditions, and having a 9% slope [12]. The C -factor is a ratio of soil loss from an area with a specified cover and management to that from an identical area under tilled continuous fallow conditions [12], and the P -factor is the ratio of soil loss with a support (conservation) practice like terracing to that with straight-row farming up and down the slope [12].

2.2.2. GIS-Based RUSLE Module

We used the RUSLE and SEDIMENTATION modules within the TerrSet GIS software to estimate reservoir sedimentation. Figure 3 is a schematic of the TerrSet GIS-based implementation of RUSLE. The GIS-based RUSLE requires spatially distributed data for inputs to Equation [1], and a DEM. A 2 m horizontal resolution DEM was derived for each watershed from airborne LiDaR image of the study area acquired with the USDA-NRCS. The regional image was downloaded from the USDA-NRCS Geospatial Data Gateway [36] from which each watershed was delineated and clipped. The RUSLE module uses the DEM to calculate the spatially distributed LS factors. The K -factor images for the watersheds were downloaded from the USDA Web Soil Survey website [35], clipped and resampled to match their respective DEM image characteristics. The R -factor image for each watershed

was created in TerrSet by first developing a “blank” image having the same file attributes (rows, columns, upper left and lower right image coordinates, map projection, etc.) as the watershed’s DEM. Initial pixels values for the R-factor image were set equal to 0. Using the OVERLAY module in the mathematical operations tool, the 1981 C-factor image was “added” to the newly created R-factor image, whose pixels values outside the watershed boundary remained 0. Pixel values within the watershed boundary were reclassified to a value of 225, which is the value for our study area based on the isoerodent map in Renard et al. [12]. The P-factor image for each watershed was created in the same way, except that the pixel values within the watershed boundary were set to a value of 1, as this is the recommended value when the support practice(s) used is/are unknown.

Within the GIS-based RUSLE, the software partitions the landscape into homogeneous patches based on user-supplied values for slope and aspect threshold. The maximum slope length parameter represents the distance that water can flow, in sheet form, before becoming concentrated, whereas the smallest-patch-size-allowed parameter allows patches below the specified value to be merged into larger patches. In our implementation of the model, we specified a slope threshold of 3%, an aspect threshold of 45°, a maximum slope length of 121.92 m, and the smallest patch size allowed of 40,468.6 m².

The SEDIMENTATION module uses the patch ID number and patch total soil loss images derived using RUSLE together with the watershed DEM and a sediment delivery ratio (SDR) to simulate and quantify net soil movement between patches. The SDR is applied at the patch level and the amount of soil loss between the higher and lower patch is proportional to the length of the common boundary between them. Patch level values are then summed to produce a net soil loss or deposition for the study unit. This value is multiplied by the reservoir study impoundment period to produce an estimate of reservoir sedimentation. Supplemental Figures S1–S12 show the slope, K-factor, RUSLE total soil loss by patch, and net soil loss from the SEDIMENTATION module of each watershed as used in the GIS-based analysis for 1981.

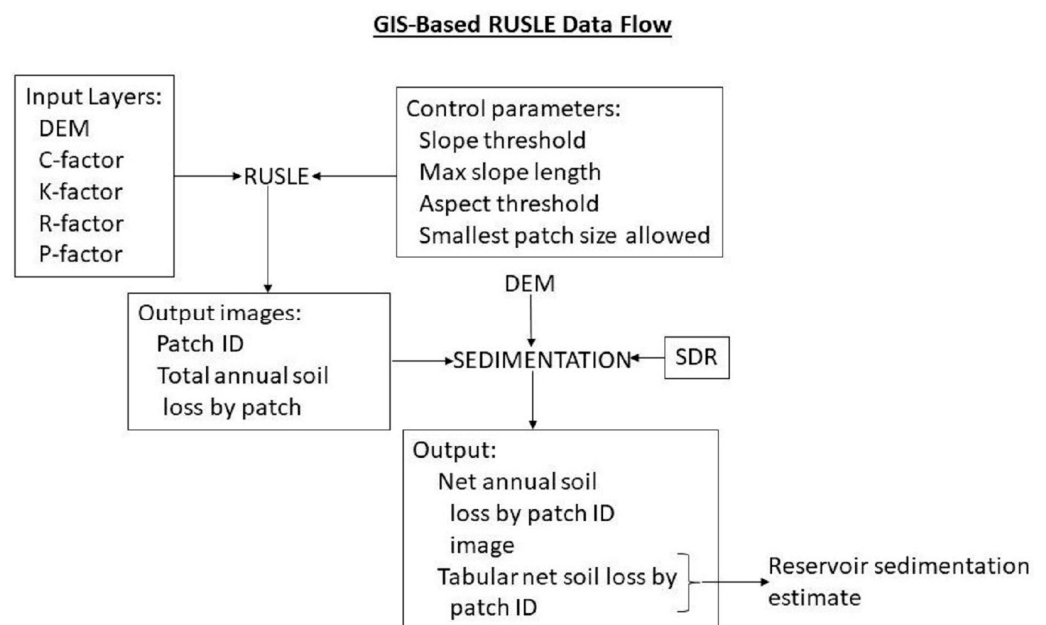


Figure 3. Schematic of the TerrSet GIS-based implementation of RUSLE and SEDIMENTATION for estimating reservoir sediment accumulation.

2.2.3. GIS-Based RUSLE Inputs

For this study, we selected five dates (1981, 1985, 1989, 1994, and 1997) of land cover data previously developed for the study area [37] to estimate the long-term reservoir sediment accumulation. These dates were selected based primarily on the availability of

land cover images for each of the study watersheds. Additionally, weather records for the LWREW indicated that rainfall varied from 90 to 120% of normal over the 1981–1997 period, which is representative of the area. Supplemental Table S5 provides a summary of the satellite sensors, the horizontal spatial resolution of the images, and the classification methods used to generate the land cover data sets. Additional details regarding the development of the land cover data sets are provided by Starks et al. [37]. The findings in [37] indicated that the LWREW is largely composed of grasslands (~65%) with ~16 and 13% of crops and tree/shrub, respectively. However, annual variations in these cover categories were observed in the study. The original land cover designations for these images were reclassified into either crop, grass, or tree/shrub categories. The dominant crop in this region is conventionally tilled winter wheat that is generally used as a forage for grazing cattle. We used a C-factor of 0.37 to represent this condition as suggested by the USDA-NRCS for this region of Oklahoma [38]. The C-factors for the grass and tree/shrub conditions were derived from the tabular data presented in Wischmeier and Smith [13]. The grasslands in the study area are highly variable in terms of vegetation type (native grasses vs. improved pastures), density of plants, and grazing pressure (lightly to heavily grazed). For grass lands, an average C-factor of 0.16 was used to represent the range of vegetative canopy cover types (grass, grass-like, and short brush), having at least 20% of the cover in contact with the soil surface. For the tree/shrub conditions, an average C-factor of 0.28 was used, which represented areas having appreciable brush, bushes, and trees with an average drop fall height of ~2 m, and with about 75% of the ground surface covered by the canopy. As noted above, the RUSLE support practice (P-) factor was set to 1, and the rainfall/runoff (R-factor) was set to 225. The P- and R-factors remained fixed over each year of analysis and were identical for each watershed. The slope length (L) and steepness (S) (combined into the LS) factors also remained unchanged for a given watershed over time. The LS values are calculated within the GIS model and are not provided herein.

2.2.4. SDR Models

The SDR is the ratio of sediment yield (SY) to total soil erosion (SE), where SY is the portion of SE that reaches the stream and transported via waterways to the reservoir. Measured values of SY and SE are not generally available for most small watersheds but can be estimated from similar watersheds where measured values are available. For this study, the sediment volumes, given in Table 2, are the SY measurements (over the impoundment period of interest), but no direct measurements of SE are available. One could use the RUSLE estimates of SE together with the measured SY values to arrive at SDR. However, we could not use this approach since we would be using RUSLE influenced SDR to evaluate RUSLE itself. Thus, an independent method of estimating SDR was needed.

The SDR can be estimated from models that relate to watershed characteristics such as W_A , W_{VL} , and watershed relief, or one could use SDRs generated from similar (in size, topographic characteristics, land cover, etc.) watersheds. Garbrecht [39] used the equation of Maner [40] to calculate the SDR for four watersheds within the nearby Fort Cobb Reservoir watershed and obtained values ranging from 0.0728 to 0.1145 (mean value of 0.1). Although these watersheds are in the same region as the ones used in this study, their areas are one to two orders of magnitude larger; thus, the mean SDR value for these four watersheds may not be representative of our study watersheds. The Maner [40] equation is as follows:

$$\text{Log}(\text{SDR}\%) = 2.94259 - 0.82362 \times \text{Log}\left(\frac{W_{vl}}{W_{rlf}}\right) \quad (2)$$

Equation (2) was applied to the study watersheds and the results reported in Table 2. We also computed the SDR from the models of USDA [41] (Equation (3)), Boyce [42] (Equation (4)), and Vanoni [43] (Equation (5)), all of which are related to W_A .

$$\text{SDR} = 0.5656 \times W_A^{-0.11} \quad (3)$$

$$SDR = 0.3750 \times W_A^{-0.2382} \quad (4)$$

$$SDR = 0.4724 \times W_A^{-0.125} \quad (5)$$

where W_A is in km^2 . The results of these equations are also provided in Table 2.

Table 2. Sediment delivery ratio (SDR) values for each watershed calculated using Equations (2)–(5).

Watershed ID	SDR Models			
	Equation (2)	Equation (3)	Equation (4)	Equation (5)
11	0.254	0.474	0.257	0.387
14	0.260	0.435	0.213	0.351
20	0.248	0.458	0.238	0.372
21	0.372	0.504	0.293	0.415
22	0.364	0.503	0.291	0.414
23	0.268	0.511	0.302	0.421
24	0.229	0.456	0.236	0.37
26	0.103	0.411	0.188	0.329
31	0.179	0.408	0.186	0.327
39	0.255	0.461	0.242	0.375
41	0.321	0.524	0.318	0.433
42	0.395	0.527	0.322	0.436

As observed from Table 2, the four models produced a wide range of values for a given watershed. The GIS-based RUSLE model (for all watersheds and dates) was run for each SDR model, and the resulting sedimentation estimates (ND_{Res} ; see Equation (6) below) were compared. Example images of RUSLE total annual soil loss by patch and SEDIMENTATION net annual soil loss by patch are provided in Supplemental Figures S1–S12. Although Equation (2) resulted in the smallest mean ND_{Res} value (Table 3), it also had the largest standard deviation. Based on the findings provided in Table 3, SDR values computed via Equation (3) were chosen, as they produced the smallest standard deviation between estimated and measured reservoir sedimentation (Table 3).

Table 3. Descriptive statistics (n -size = 12 watersheds \times 5 yr/watershed, mean, standard deviation, coefficient of variation (CV), and minimum and maximum values) of the normalized difference between GIS-based RUSLE estimated and measured reservoir sedimentation (ND_{Res} ; see Equation (6)) using the SDR calculated from Equations (2)–(5).

SDR	n-Size	ND_{Res} (%)				
		Mean *	Std. Dev.	CV	Min	Max
Equation (2)	60	−40.2 ^{ab}	104.9	261.1	−96.9	548.2
Equation (3)	60	−61.9 ^b	66.6	107.6	−97.8	332.8
Equation (4)	60	−45.6 ^{ab}	94.6	207.5	−96.9	518.7
Equation (5)	60	−54.9 ^{ab}	78.3	142.5	−97.4	412.6

* Means not connected by the same letter are significantly different ($\alpha = 0.05$).

2.3. Normalized GIS-Based RUSLE Reservoir Sedimentation Estimates

Average annual soil loss was determined for each watershed for each of the five years. The annual soil losses were multiplied by the respective reservoir's impoundment period (Table 2) and sediment bulk density [1] to estimate reservoir sedimentation for comparison against measured values (Table 2). The resulting estimated sedimentation values were normalized (ND_{Res}) with reference to the measured sedimentation data acquired from the bathymetric survey for the respective reservoir according to the following:

$$ND_{Res} = \frac{\text{Estimated Sedimentation} - \text{Measured Sedimentation}}{\text{Measured Sedimentation}} \times 100, \quad (6)$$

where positive values of ND_{Res} indicate percentage overestimation relative to the measured values and negative values indicate percent underestimation.

2.4. Stream Bank Sediment Contributions

2.4.1. First-Order Adjustment

Ref. [27] showed, for a stream near our study area, that ~54% of the suspended sediment in stream flow was due to stream bank sources. Assuming that this finding is applicable to other streams near the study region, the measured reservoir sediment values were decreased by 54% before comparing them against GIS-based RULSE estimates.

2.4.2. Statistical Linkages between ND_{Res} and Watershed, Stream, Stream Corridor, and Within-Channel Variables

In contrast to the regional adjustment approach in Section 2.4.1, we developed watershed, stream, stream corridor, and within-channel variables (described below) as possible indicators of sediment contributions from gullies, stream banks, or stream channels.

2.5. Statistical Analysis

The various data types (RUSLE inputs, watershed, stream, stream corridor, within-channel, and ND_{Res}) were analyzed in JMP 17 Pro (SAS Institute, Cary, NC, USA) to produce basic descriptive statistics and to evaluate differences between estimated and measured sedimentation as a function of year of land cover (C-factor) acquisition, subdominant land cover, and other variables, and for identifying variables that may be predictive of the discrepancy between measured and modeled reservoir sedimentation. All non-normal data were transformed before analysis.

3. Results and Discussion

3.1. Variability in RUSLE C- and K-Factors

3.1.1. C-Factors (Land Cover)

Satellite data from five dates were used to quantify land area within a given watershed in either crops, grass, tree/shrub, or fallow. It was expected that small changes in land cover area between years would occur, but the actual magnitude of these changes and their impacts on the estimates of reservoir sediment accumulation were unknown. An example of temporal variability of land cover within Watershed 24 is provided in Table 4 where it is observed that watershed area associated with trees/shrubs increased from ~6% in 1981 to ~9% in 1989 but occupied ~4% of the watershed area in 1994 and 1997. The largest temporal changes occurred in the cropland and grassland subdominant land cover groups. This is not uncommon in areas where some agricultural producers may shift from grazing livestock to planting alfalfa, cereal grains, or other crops, or conversely, where some cropland may be converted back to grassland, possibly to take advantage of changing cattle markets or to participate in conservation programs. An example of such a large temporal change in the crop and grass groups is observed in 1989, whereas in the years prior to this, cropland accounted for 41 to 47% of the watershed area. However, that percentage was greatly reduced in 1989 when cropland accounted for ~18% of the watershed area. Fallow ground was observed in 1981 and 1985, but the percentage of watershed areas was less than 1%. Large temporal changes between cropland, grassland, and tree/shrub lands are observed for other watersheds in this study (Figure 4 and Supplemental Table S6). Fallow ground was < 6.3% in all watersheds but averaged ~0.7% across all watersheds and satellite land cover dates (Supplemental Table S6).

The C-factor values are directly linked to the cover type; thus, Table 4 (and Supplemental Table S6) can also be interpreted as the total watershed area associated with a given C-factor. The largest C-factor (1) is associated with fallow ground, which occupies a small area in Watershed 24 (Table 4). However, the cropped area (C-factor = 0.37) ranged from 18 to 47%. Thus, it could be expected that soil erosion was highest in 1989, depending upon timing, amount, and rates of rainfall during that

year, all other things being equal. The C-factor associated with the tree/shrub category (C-factor = 0.28) occupied from ~4 to ~9% of the watershed area, depending on year, whereas the C-factor associated with the grass category (C-factor = 0.16) varied from ~48% to ~75% of the watershed’s total area. Watershed C-factor images for each of the five dates are provided in Supplemental Figures S13–S24.

Table 4. Decimal percentage of total watershed area, by year, under either crop, grass, tree/shrub, or fallow ground, for Watershed 24.

Cover Type	Image Year				
	1981	1985	1989	1994	1997
Crop	0.471	0.414	0.179	0.394	0.445
Fallow	--	0.002	0.005	--	--
Grass	0.488	0.544	0.752	0.594	0.537
Tree/Shrub	0.064	0.064	0.088	0.035	0.042

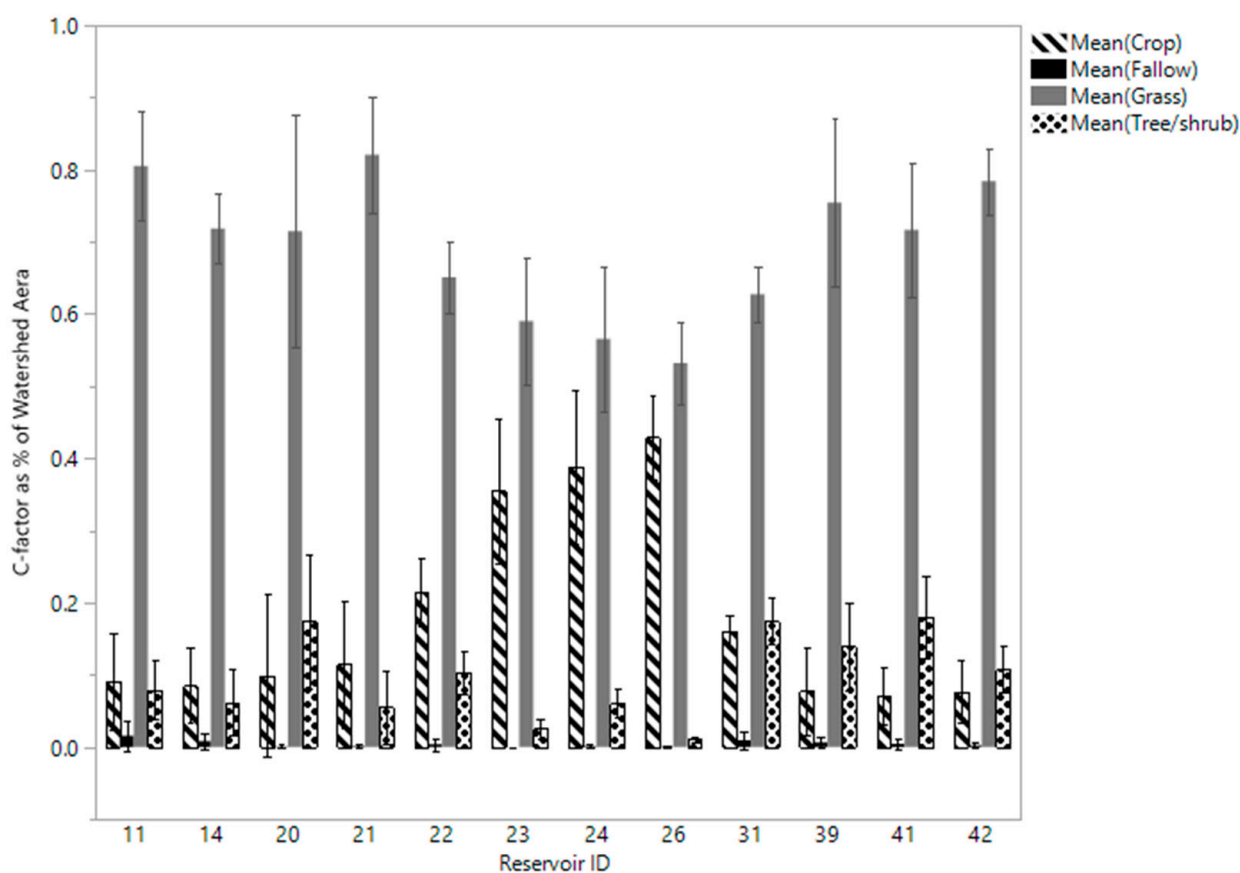


Figure 4. Mean of total watershed area under a given C-factor (or land cover type) for the watershed indicated. One standard deviation is indicated for each bar.

3.1.2. K-Factors

The soil erodibility (K-) factors are different in value, distribution, and number for each watershed but remained static for a given watershed regardless of the year of analysis (Table 5, Supplemental Figures S1–S12). Zero (0) values indicate no soil erodibility and correspond to percentage of water surface in each watershed. Such values could also indicate impervious surfaces, but surfaces of this type were not apparent in the K-factor data. It is readily observed from Table 5 that Watersheds 22, 23, 24, 26, and 31 have $\geq 55\%$ of their areas in soils with K-factors ≥ 0.37 (moderate to highly erosive soils). Watershed

11 has ~31% of its area in these moderate to highly erosive soils, whereas the remaining watersheds have ≤ 14%. Watershed area-weighted K-factors ranged from 0.16 (Watershed 14) to ≥ 0.30 for Watersheds 22, 23, 24, 26, and 31.

Table 5. Decimal percentage of watershed area in water and a given K-factor shown with respect to watershed ID (WS ID). An area-weighted K-factor (W_K) is also shown for each watershed.

WS ID	0 (Water Area)	K-Factors as a Decimal% of Watershed Area										W_K
		0.02	0.1	0.15	0.2	0.24	0.28	0.32	0.37	0.43	0.49	
11	0.0089	0.155	0	0.233	0.288	0	0	0.008	0.077	0.116	0.115	0.23
14	0.125	0.014	0	0.242	0.619	0	0	0	0	0	0	0.16
20	0.012	0.02	0.104	0.214	0.353	0	0.156	0	0.052	0.077	0.012	0.22
21	0.008	0.064	0.131	0.2	0.314	0	0.203	0	0.059	0	0.021	0.20
22	0.04	0	0.044	0	0.098	0	0.061	0	0.417	0.182	0.158	0.35
23	0.028	0	0.0001	0.015	0.078	0	0.205	0	0.493	0.137	0.044	0.34
24	0.022	0	0	0	0.011	0.011	0.154	0	0.599	0.113	0.089	0.36
26	0.028	0	0	0	0.0005	0.001	0	0	0.743	0	0.228	0.39
31	0.027	0.001	0.01	0.002	0.093	0.088	0.222	0	0.394	0.02	0.143	0.33
39	0.022	0.032	0	0.035	0.653	0.113	0.145	0	0	0	0	0.20
41	0.025	0	0	0.333	0.642	0	0	0	0	0	0	0.18
42	0.029	0	0	0.013	0.91	0	0	0	0.024	0.007	0.017	0.20

3.2. Initial Reservoir Sedimentation Analysis

All ND_{Res} were pooled over satellite land cover date within and across the subdominant watershed landcover categories and summary statistics calculated (Table 6). From this analysis, it was observed that for all watersheds combined, the GIS-based RUSLE model underestimated accumulated reservoir sediment by ~62%, on average. However, there was a considerable difference between maximum and minimum ND_{Res} . At the subdominant land cover category level, the Crop watershed group exhibited the largest variability in ND_{Res} , ranging from an overestimation of ~333% to an underestimation of ~98% (CV = 339%). The Grass and Tree/Shrub groups exhibited smaller ranges (CVs = 64.7 and 13.6%, respectively), with average ND_{Res} values of ~-72 and -83%, respectively.

Table 6. Summary statistics of ND_{Res} by watershed subdominant land cover group and for all watersheds combined.

Statistic	Watershed Land Cover Group			
	Crop	Grass	Tree/Shrub	All
Maximum (%)	332.8	8.9	-56.1	332.8
Minimum (%)	-97.5	-93.4	-97.8	-97.8
Mean (%)	-31.4	-71.7	-82.9	-62.0
Std. Dev. (%)	106.5	27.0	12.2	66.6
N-size	20	20	20	60

Further analysis indicated that the annual estimates of reservoir sedimentation were not normally distributed. These data were subsequently normalized (ND_{ResT}) using a Johnson SU transformation [44]. After the transformations, the data were subjected to ANOVA and Student’s *t*-test to further investigate any statistical differences in the subsequent estimates of ND_{Res} and ND_{ResT} as a function of land cover date used to determine the C-factors, and to investigate differences in ND_{Res} within and across watershed subdominant land cover group, and across individual watersheds.

3.3. Effects of Land Cover (C-factor) Date on Sedimentation Estimates

3.3.1. Date Effects Pooled over All Watersheds

ANOVA of the ND_{ResT} data indicated that the various satellite dates did not produce statistically significantly different estimates of sedimentation ($p = 0.6352$). Student’s *t*-test further corroborated the ANOVA results (Table 7). In practical terms, however, if the 1985

C-factors were used to estimate the long-term reservoir sedimentation, this would produce an average underestimation of reservoir sedimentation of ~42%, while the 1994 land cover data would have produced an average underestimation of ~79%

3.3.2. Date Effects within Watershed Subdominant Land Cover Group

ANOVA of the ND_{ResT} data indicated no statistically significant effects of year of land cover date within either the Crop or Grass subdominant land cover categories ($p = 0.4482$ and 0.68901 , respectively). Student's t -test further corroborated the ANOVA results (Table 7). However, the ANOVA for the Tree/Shrub group of watersheds did indicate that at least one of the land cover dates produced estimates of ND_{ResT} that were statistically different from estimates generated from one or more of the other dates. According to the t -test, the C-factors generated from the 1985 land cover data were statistically distinct from that generated using the 1989 land cover data.

In practical terms, estimated reservoir sedimentation within the reservoirs assigned to the Crop category of watersheds ranged from an overestimation of ~27% in 1985 to an underestimation of ~76% in 1981. For reservoirs within the Grass group, all years were associated with underestimates of measured reservoir sedimentation, ranging from -81% (1985) to -58% (1997). Similarly, all model simulations of reservoir sedimentation in the Tree/Shrub category of watersheds underestimated measured values, ranging from -91% (1989) to -71% (1985).

Table 7. Least square means * of ND_{ResT} as a function of land cover/C-factor date within the subdominant landcover groups.

Date	All	Crop	Grass	Tree/Shrub
1981	0.438	0.510	0.481	0.323 ^{ab}
1985	0.545	0.618	0.422	0.593 ^a
1989	0.499	0.843	0.462	0.193 ^b
1994	0.454	0.565	0.401	0.395 ^{ab}
1997	0.595	0.738	0.667	0.369 ^{ab}

* ND_{ResT} means not connected by the same letter are significantly different ($\alpha = 0.05$).

3.4. Comparison of Averaged Estimated and Measured Reservoir Sedimentation

Although not statistically significant, given the large practical differences between estimated and measured reservoir sedimentation, the analyses reported below are based on the GIS-based RUSLE simulations for all years and watersheds.

3.4.1. Between Subdominant Land Cover Groups

The ANOVA of ND_{ResT} , pooled over date within watershed subdominant land cover groups (Table 8), indicated that at least one watershed land cover group represented a different population ($p = 0.004$). Figure 3 indicates that the corresponding ND_{Res} values are more variable over time for Crop watersheds than those for the Grass and Tree/Shrub watersheds. Although the ND_{ResT} for the Grass and Tree/Shrub groups are statistically similar, the Tree/Shrub group's standard deviation is about half of that of the Grass watershed group. On average, the estimated reservoir sedimentation from the Crop, Grass, and Tree/Shrub watersheds underestimated measured values by 31, 71, and 83%, respectively (Figure 5).

Table 8. Results of Student's *t*-test on ND_{ResT} , pooled over date within watershed subdominant land cover group.

Watershed Land Cover	* ND_{ResT} Least Square Mean
Crop	0.655 ^a
Grass	0.489 ^b
Tree/shrub	0.374 ^b

* Means not connected by the same letter are significantly different ($\alpha = 0.05$).

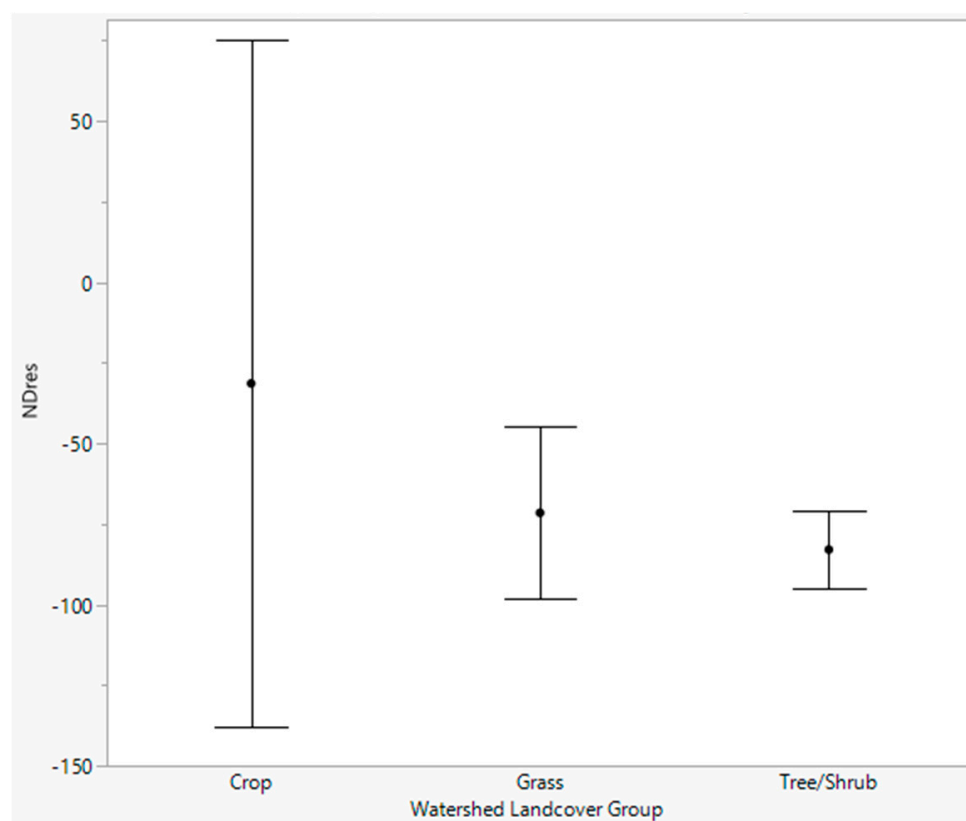


Figure 5. Plot of mean ND_{Res} (solid circle) by watershed subdominant land cover group. Error bars indicating one standard deviation above and below the mean value are also shown.

3.4.2. Between Reservoirs within Subdominant Land Cover Group

ANOVA of average watershed ND_{ResT} within the Crop and Grass subdominant land cover groups indicated that at least one watershed within each group produced a ND_{ResT} that represented a different population when compared to other watersheds within the group ($p = 0.03$ and 0.01 , respectively). The ANOVA for the Tree/Shrub group indicated that the watershed ND_{ResT} estimates were all drawn from the same population ($p = 0.4442$). Student's *t*-test (Table 9) indicated that, in the Crop watershed group, the ND_{ResT} for Watershed 31 was statistically different from the remaining watersheds within the group. The Grass group watersheds exhibited more statistical differences among themselves than those observed for the other two subdominant land cover watershed groups. In the Grass group, it was observed that Watershed 11 generated ND_{ResT} values that were statistically different from those for Watersheds 21 and 14, whereas Watershed 14 values were statistically dissimilar to Watersheds 11 and 22.

Table 9. Results of Student's *t*-test on watershed least square means of ND_{ResT} within watershed landcover group.

Crop		Grass		Tree/Shrub	
Watershed ID	ND _{ResT} *	Watershed ID	ND _{ResT}	Watershed ID	ND _{ResT}
24	0.809 ^a	11	0.726 ^a	41	0.476
23	0.743 ^a	22	0.589 ^{ab}	39	0.417
26	0.681 ^a	21	0.370 ^{bc}	42	0.383
31	0.387 ^b	14	0.269 ^c	20	0.222

* ND_{ResT} means not connected by the same letter are significantly different ($\alpha = 0.05$).

The actual ND_{Res} values for the Crop group of watersheds indicate that reservoir sedimentation estimates ranged from an underestimation of ~83% (Watershed 31) to an overestimation of ~24% (Watershed 23). All model simulations underestimated reservoir sedimentation for all watersheds within the Grass group and ranged from ~−50% (Watershed 11) to ~−89% (Watershed 14). Model simulations for the Tree/Shrub watersheds underestimated measured values for all watersheds and ranged from ~−77% (Watershed 41) to ~−89% (Watershed 20).

3.4.3. Across All Watersheds

The ANOVA indicated that ND_{ResT} of at least one watershed represented a different population ($p = 0.0004$). Results of the Student's *t*-test are provided in Table 10, where values shown in the table are the same as those provided in Table 9 but are ranked with respect to each other.

Table 10. Results of Student's *t*-test performed on the least square means of ND_{ResT} pooled over year of satellite land cover/C-factor dates within watershed.

Watershed/Reservoir ID	Watershed Subdominant Land Cover Group	* ND _{ResT}
24	Crop	0.809 ^a
23	Crop	0.743 ^{ab}
11	Grass	0.726 ^{ab}
26	Crop	0.681 ^{abc}
22	Grass	0.589 ^{abcd}
41	Tree/shrub	0.476 ^{bcde}
39	Tree/shrub	0.417 ^{cde}
31	Crop	0.387 ^{de}
42	Tree/shrub	0.383 ^{de}
21	Grass	0.370 ^{de}
14	Grass	0.269 ^e
20	Tree/shrub	0.222 ^e

* ND_{ResT} means not connected by the same letter are significantly different ($\alpha = 0.05$).

Watershed 23 was the only 1 of the 12 watersheds that produced a positive mean ND_{Res} value (Figure 6). However, this watershed exhibited the most variable results (Figure 6), followed closely by Watershed 24. The high variability in these two watersheds (both members of the Crop subdominant land cover group) is due to a single comparatively high ND_{Res} value. For Watershed 23, a ND_{Res} of over 300% occurred in 1985, whereas a value of nearly 200% for Watershed 24 occurred in 1989. Removal of these two data points brings the mean ND_{Res} values to −53.4% for Watershed 23, and to −56.0% for Watershed 24 (Table 11). Although the prior Crop watershed mean ND_{Res} was negative (Table 6), it became more negative (−64.4%; calculated from the values provided in Table 11) with the removal of these two data points, bringing the subdominant land cover group of reservoir's ND_{Res} average in closer agreement with that of the Grass and Tree/Shrub group.

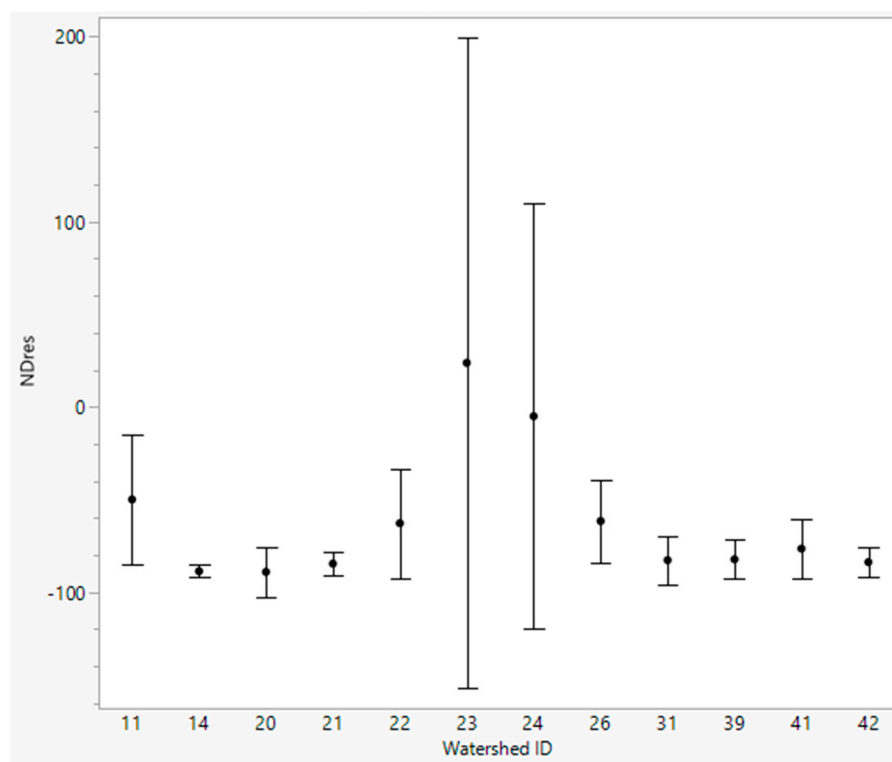


Figure 6. Plot of mean normalized difference (solid circle) between estimated and measured reservoir sediment accumulation by watershed. Error bars indicating one standard deviation above and below the mean value are also shown.

If the ND_{Res} values generated from the 1985 and 1989 dates for Watersheds 23 and 24, respectively, are outliers, then reanalysis of the data set indicates that the overall average underestimation of reservoir sedimentation is $72.6\% \pm 14.8\%$, and that the watershed mean ND_{Res} values range from -50% (Watershed 11) to -89.2% (Watershed 14) (Table 11). From inspection of the ND_{ResT} values and their statistical similarity designations, two broad groups emerge and are as follows: Group 1 (all connected by the letter “a”) consisting of Watersheds 11, 22, 23, 24, and 26, and Group 2 (all connected by the letter “e”) consisting of Watersheds 14, 20, 21, 31, 39, 41, and 42 (Table 12). The ND_{Res} mean for Group 1 is $-56.8 \pm 5.4\%$, and the Group 2 mean is $-84.0 \pm 4.3\%$. The Group ND_{Res} means are statistically different at the $\alpha = 0.05$ level.

3.5. Stream Bank Contributions—First-Order Adjustment

The results of this adjustment ($ND_{Res,adj}$) are provided in the right-most column of Table 11, where it is observed that the discrepancy between the estimated and measured values of reservoir sedimentation for Reservoirs 11, 22, 23, 24, and 26 was under 20% (absolute), averaging $-6.0 \pm 11.8\%$. However, the $ND_{Res,adj}$ for the remaining seven watersheds ranged from -49.0% (Reservoir 41) to -76.3% (Reservoir 20). It was observed that $ND_{Res,adj}$ for Reservoir 41 was more statistically like Group 2 (ending statistical similarity designator = e) than Group 1 (ending statistical similarity designator = d). The mean ND_{Res} for Group 2 is $-65.1 \pm 9.3\%$. The difference between the two groups after adjusting for stream bank contributions suggested that a regionally based adjustment for gully or stream bank sediment contributions would not be sufficient to account for RUSLE’s weakness in this area. Thus, further analysis was needed to identify watershed, stream, stream corridor, or within-channel characteristics that may be used as proxies to account for sediment contributions derived from gullies, stream channels, or stream banks.

Table 11. Results of Student's *t*-test performed on the ND_{ResT} pooled over year excluding two "outlier" land cover/C-factor dates and their associated mean ND_{Res} and the ND_{Res} adjusted for first-order contribution of steam bank/channel sedimentation (ND_{Res_adj}) for each watershed.

Watershed/Reservoir ID	Watershed Land Cover Group	* ND_{ResT}	ND_{Res} Mean (%)	ND_{Res_adj} Mean (%)
24	Crop	0.763 ^a	−56.0	−4.3 ^{abc}
11	Grass	0.726 ^b	−50.0	8.7 ^a
26	Crop	0.681 ^{ab}	−61.6	−16.6 ^{abcd}
23	Crop	0.679 ^{abc}	−53.4	1.4 ^{ab}
22	Grass	0.589 ^{abcd}	−62.8	−19.2 ^{abcd}
41	Tree/shrub	0.476 ^{abcde}	−76.5	−49.0 ^{bcde}
39	Tree/shrub	0.417 ^{bcde}	−82.3	−61.5 ^{cde}
31	Crop	0.387 ^{cde}	−82.7	−62.5 ^{cde}
42	Tree/shrub	0.383 ^{cde}	−83.8	−64.8 ^{de}
21	Grass	0.370 ^{de}	−84.6	−66.6 ^{de}
14	Grass	0.269 ^e	−88.9	−75.9 ^e
20	Tree/shrub	0.222 ^e	−89.1	−76.3 ^e

* ND_{ResT} least square means followed by different letters are significantly different ($\alpha = 0.05$) (the data used to derive the ND_{Res} values provided in Table 11 are used in the analyses reported in subsequent sections).

3.6. Watershed, Stream, Stream Corridor, and Within-Channel Variables

3.6.1. Watershed and Stream Variables

Generally, the watersheds are of moderate-to-low relief with an average basin relief of ~51 m and range from a high of ~78 m (Watershed 31) to a low of 38 m (Watershed 21) (Supplemental Table S7). The $\%W_{slope \geq 21}$ varied from a low of 0.3% (Watersheds 39 and 41) to a high of 9.7% (Watershed 22), averaging $\sim 2.3 \pm 2.7\%$ across all watersheds. The W_{vl} averaged 4135 m across all watersheds but is quite variable ranging from 1761 m (Watershed 21) to 11,002 m (Watershed 26). Similarly, S_{thal} varied from 13,196 m (Watershed 31) to 1844 m (Watershed 21), averaging 4939 ± 3406 m. The S_{slope} were gentle for all watersheds, averaging 0.013 ± 0.005 m m^{-1} , while S_{sn} values indicated that five of the streams are essentially straight ($S_{sn} < 1.05$), while the remaining seven streams have low sinuosity ($1.06 > S_{sn} \leq 3.0$).

Watershed topographic and general stream characteristics are presented in Table 12 where it is observed that the two groups are statistically similar in terms of W_A , W_{rlf} , $\%W_{slope \geq 21}$, S_{thal} , S_{slope} , and S_{sn} . However, the two groups statistically differ in percent of watershed area in $\%W_{LK}$, $\%W_{MK}$, and $\%W_{HK}$. Watersheds in Group 2 have, on average, ~74% of their areas in $\%W_{LK}$ with about 72% of these soils having a value ≤ 0.2 (Table 5). Watersheds in Group 1 have ~66% of their areas in $\%W_{MK}$, with ~47% of these soils having a value ≥ 0.37 (Table 5). Additionally, Group 1 watersheds have another 13% of their areas in high K-factor soils, indicating that Group 1 watersheds have more erosive soils than those observed in the Group 2 watersheds.

3.6.2. Stream Corridor Variables

The $\%Cor_{slope \geq 21}$ ranged over two orders of magnitude from 0.6% (Watershed 39) to 9.7% (Watershed 42) and to 36.8% (Watershed 21) (Supplemental Table S8). The $\%Cor_{slope \geq 21}$ for Watersheds 21, 23, and 31 averaged $28.5 \pm 12.7\%$, and it averaged $5.5 \pm 3.3\%$ over the remaining watersheds. The $Cor_{slope \geq 21}:W_{VL}$ varied from 1.8 m^2m^{-1} (Watershed 41) to 36.8 m^2m^{-1} (Watershed 22), averaging 9.5 m^2m^{-1} over the 12 study sites (Supplemental Table S8). The $\%Cor_{LK}$, $\%Cor_{MK}$, and $\%Cor_{HK}$ variables averaged 47.6, 48.4, and 4.0%, respectively, over the study sites. However, considerable variability was observed between sites for all three K-factor categories. For example, the corridors in Watersheds 14 and 41 had 100% of their areas in low K-factor soils, whereas Watersheds 24 and 26 had 5.8 and 0.3%, respectively (Supplemental Table S8). Moderate K-factor soils occupied $\geq 70\%$ of corridor areas in Watersheds 21, 22, 23, 24, 26, and

31. High K-factor soils were not present in the corridors of Watersheds 11, 14, 21, 39, and 41 and accounted for $\leq 5\%$ in Watersheds 22, 23, 31, and 42. Watershed 26 had the largest corridor area in high K-factor soils at $\sim 26\%$.

Table 12. Comparison of Group 1 and 2 least square means of watershed area (W_A), watershed basin relief (W_{rif}), percent of watershed area with slopes $\geq 21^\circ$ ($\%W_{slope>21}$), percentage of watershed area in low, moderate, or high K-factor soils ($\%W_{LK}$, $\%W_{MK}$, and $\%W_{HK}$), stream thalweg length (S_{thal}), stream slope (S_{slope}), and stream sinuosity (S_{sn}).

Broad Group ID	Watershed Variables *							Stream Variables			
	W_A (km ²)	W_{rif} (m)	$\%W_{slope\geq 21}$	W_{vl}	$\%W_{LK}$	$\%W_{MK}$	$\%W_{HK}$	W_K	S_{thal} (m)	S_{slope} (m m ⁻¹)	S_{sn}
1	7.1	51.0	1.7	5101	19 ^b	66 ^a	13 ^a	0.33 ^a	6078	0.011	1.21
2	7.1	51.5	1.0	3753	74 ^a	19 ^b	3 ^b	0.21 ^b	4124	0.015	1.09

* Means not connected by the same letter are significantly different ($\alpha = 0.05$).

Low K-factor soils in the 100 m stream corridor ($\%Cor_{LK}$) are statistically and significantly more prominent in the Group 2 watersheds ($\sim 67\%$) than in Group 1 watersheds ($\sim 20\%$) (Table 13). Conversely, $\sim 80\%$ of the Group 1 corridor is in moderate-to-high K-factor soils. The $\%Cor_{slope\geq 21}$ is statistically similar between groups, but in practical terms, the Group 2 watersheds have twice their corridor areas occupied by slopes $\geq 21^\circ$ as compared to the Group 1 watersheds. Interestingly, however, $Cor_{slope>21}:W_{vl}$ is statistically and practically higher in Group 1 corridors containing about three times more area with slopes $> 21^\circ$ per m of W_{vl} . This variable may be an indicator of bank instabilities and/or development of gullies along the main channel of the stream and its tributaries, and therefore, they are potential sources of sediments for which the GIS-based RUSLE cannot account.

Table 13. Comparison of Group 1 and 2 100 m stream corridor least square means of low, moderate, and high K-factor soils ($\%Cor_{LK}$, $\%Cor_{MK}$, and $\%Cor_{HK}$, respectively), slopes $\geq 21^\circ$ ($\%Cor_{slope>21}$), and ratio of corridor slope area $> 21^\circ$ ($Cor_{slope>21}$) to watershed valley length ($Cor_{slope>21}:W_{vl}$).

Group ID	Soil K-Factor *			Topographic *	
	$\%Cor_{LK}$	$\%Cor_{MK}$	$\%Cor_{HK}$	$\%Cor_{slope>21}$	$Cor_{slope>21}:W_{vl}$ (m ² m ⁻¹)
1	19.8 ^b	71.9 ^a	8.3 ^a	7.7	15.4 ^a
2	67.4 ^a	31.6 ^b	1.0 ^b	13.8	5.2 ^b

* Means not connected by the same letter are significantly different ($\alpha = 0.05$).

3.6.3. Within-Channel Variables

The BFD varied from 0.22 m (Watershed 42) to 1.29 m (Watershed 31), averaging 0.6 m over all 12 study sites (Supplemental Table S9). On average, the BFW was about 40 times the BFD but varied from ~ 13 (Watershed 23) to ~ 99 (Watershed 11) times larger than the BFD (see BFW:BFD in Supplemental Table S9). The BAs were found to be low for all streams as they were generally $\leq 20^\circ$ (Supplemental Table S9). Average BH was 2.4 m, which is categorized as very high (Supplemental Tables S3 and S7), but varied from 0.65 (Watershed 11) to 4.14 m (Watershed 22). Of the 12 study sites, BH was ≥ 2.1 m (very high, Supplemental Table S3) for all but Watersheds 14, 39, 41, and 42. The BHR averaged 4.5, which is classified as highly unstable (Supplemental Tables S2 and S9). The BHR value for all sites indicated that all stream banks were unstable (Supplemental Tables S2 and S9). The ER for all streams indicated that they were slightly to moderately entrenched as ER was generally ≥ 1.4 (Supplemental Tables S4 and S9), with an overall average of 3.5. On average, CD was 2.9 m, CW was ~ 38 m, and CA was ~ 80 m². However, CD, CW, and CA varied considerably (Supplemental Table S9).

The two groups are statistically similar with regard to CD, CW, CW:CD, and CA (Table 14). However, the stream channels are, on average, about 1.2 m deeper in Group 1

than those in Group 2. This difference in CD accounts for the rather large disparity, although not statistically significant, between the CW:CD values, i.e., for Group 1, the mean stream CW is ~18 times the CD, whereas the CW for Group 2 is ~36 times the CD. The CA of the Group 1 streams is ~1.5 times larger than that of Group 2. Except for BHR, the stream bank variables are not statistically different between the two groups. Although not statistically different, the ER values indicate that Group 1 streams are moderately entrenched, whereas Group 2 streams are slightly entrenched (Table 15 and Supplemental Table S4). For Group 1, the ER suggests that the streams are somewhat disconnected from their floodplains; thus, sediments derived from various sources are likely to stay within the streams and be more efficiently moved to the receiving reservoir. Conversely, the streams in Group 2 are more connected to their floodplains; thus, sediments derived from various sources could be re-deposited within the floodplain increasing their residence time within the watershed before ultimately being deposited into the receiving reservoir. The BA values are classified as low (Supplemental Table S3) for both groups and are not statistically different. The BH values are also not statistically different between the two groups; however, BH for the Group 1 streams is classified as “extreme”, while it is classified as “high” for Group 2 streams (Supplemental Table S3). The Group BHR values are statistically different, and both values indicate highly unstable banks (Supplemental Table S1)—but more so for streams in Group 1. The BA, BH, and BHR data indicate that the banks and channels in Group 1 likely contribute more sediments to their streams than do the stream banks in Group 2. Group means of FWA_%WA were not statistically different, but values ranged from a low value of 1.56 (WS 14) to 5.71 (WS 23) (Supplemental Table S9).

Table 14. Stream segment-weighted least square means of within-channel and stream bank variables of bank full depth (BFD), bank full width (BFW), ratio of BFW to BFD (BFW:BFD), bank angle (BA), bank height (BH), bank height ratio (BHR), entrenchment ratio (ER), stream channel depth (CD), stream channel width (CW), ratio of channel width to channel depth (CW:CD), channel cross-sectional area (CA), and stream horizontal surface area as a percentage of watershed area (SA_%WA) for each group.

Group ID	BFD (m)	BFW (m)	BFW:BFD	Within-Channel Variables *								
				BA (deg)	BH (m)	BHR	ER	CD (m)	CW (m)	CW:CD	CA (m ²)	FWA_%WA
1	0.65	15.3	43.2	17.9	3.0	5.8 ^a	2.1	3.6	36.1	18.0	91.3	3.7
2	0.57	15.6	38.8	12.7	2.0	3.5 ^b	4.5	2.4	38.8	36.0	70.0	2.7

* Means followed by different letters are significantly different ($\alpha = 0.05$).

Except for Watershed 26, $IC_{Sa} \geq 41\%$ (Supplemental Table S10), averaging $51.8 \pm 13.8\%$ over all sites. The IC_{Si} varied from 18% (Watershed 41) to 56% (Watershed 26). Low K-factor soils dominate in the streambed and stream banks of Watersheds 11, 14, 20, 39, 41, and 42, but moderate K-factor soils make up > 55% of the area in the remaining study sites. In fact, moderate K-factor soils make up > 91% of the streambed and stream bank soils in Watersheds 22, 24, and 26. High K-factor soils make up < 0.5% of the soils in Watersheds 20, 22, and 31 with the remaining sites having no high K-factor soils present. The plasticity index (IC_{PI}) varied from a low of 4.6 (Watershed 41) to a high of 17.3 (Watershed 26) (Supplemental Table S10).

In terms of the within-channel soils variables, the Group 1 soils have a larger silt (IC_{Si}) and smaller sand fractions (IC_{Sa}) than soils in Group 2 (Table 15). Correspondingly, the within-channel soils for Group 1 have K-factors that are predominantly (~78%) moderate in value, whereas the Group 2 stream channel and stream bank soils are predominantly (~74%) low in value. High K-factor soils accounted for < 1% of the soils in both groups, with no statistical differences between the groups. On average, the stream channel and stream bank soils in Group 1 soils have statistically larger K-factors (0.33) than those in Group 2 (0.23) and are, therefore, more erosive. The $\%IC_{PI}$ of the stream channel and stream bank soils is not statistically different between groups, although the value for Group 1 is ~1.4 times larger than that of Group 2.

Table 15. Least square means of within-channel (IC)-weighted soil K-factor (IC_K), sand (IC_{Sa}), and silt (IC_{Si}) fractions, percentages of low, moderate, and high K-factor soils ($\%IC_{LK}$, $\%IC_{MK}$, and $\%IC_{HK}$), and weighted average plasticity index (IC_{PI}) for each group's stream channels and stream banks.

Group ID	IC_K *	IC_{Sa}	IC_{Si}	$\%IC_{LK}$	$\%IC_{MK}$	$\%IC_{HK}$	IC_{PI}
1	0.33 ^a	40.8 ^b	37.2 ^a	21.6 ^b	78.2 ^a	0.14	10.9
2	0.23 ^b	59.6 ^a	23.1 ^b	73.9 ^a	25.1 ^b	0.09	7.6

* Means followed by different letters are significantly different ($\alpha = 0.05$).

3.7. Sediment Delivery Ratios (SDRs)

Setting the SDR to one forces the SEDIMENTATION module to route all RUSLE-simulated soil erosion through the watershed to the receiving reservoir, thereby providing a maximum sedimentation estimate. Comparison of GIS-based RUSLE simulations where $SDR = 1$ (all years, all watersheds) revealed that average watershed sedimentation overestimated measured values from ~1200% (Watershed 14) to ~22,000% (Watershed 23). Because the SEDIMENTATION module applies the SDR to each patch and because the amount of soil moving from one patch to the next is proportional to length of the common boundary between the two patches, sediment movement and delivery to the reservoir are reduced beyond a simple multiplication of the SDR and the RUSLE estimate of overland soil erosion. Thus, it is fortuitous that the combination of the first-order adjustment and the SDRs used in the GIS-based RUSLE simulations for the Group 1 watersheds worked as well as they did. However, this combination did not work as well for the Group 2 watersheds. The persistent and large underestimation of measured reservoir sedimentation in Group 2 watersheds after the first-order adjustment implies that the SDRs used for these watersheds are too high (i.e., too much sediment is allowed to pass through the watershed to the reservoir), or that the assumed amount of sediment generated from channels, banks, and gullies is too large. We have no information for our region than that provided by Wilson et al. [29] regarding sediments derived from channel, bank, and gully sources. Therefore, the impact of lowering the SDR to 0.1 for the Group 2 watersheds based on the study of Garbrecht [39] was investigated, while at the same time maintaining the first-order adjustment for stream channel, stream bank, and gully sediment contributions. This value for the SDR was helpful in some instances, but the underestimation remained large for some watersheds (Supplemental Table S11). Watershed 31 improved from a large underestimation to a moderate underestimation, and Watersheds 41 and 42 changed from a large underestimation of measured reservoir sedimentation to moderate overestimations (24.3 and 18.7%, respectively, Supplemental Table S11), implying that an SDR value between 0.1 and that calculated from Equation (3) could improve agreement between estimated and measured sedimentation, but without measurements of actual soil erosion, selection of the appropriate SDR would be subjective. Large underestimations were persistent for Watersheds 14, 20, 21, and 39. These findings suggest that an unrealistically small SDR would be needed to bring estimated and measured reservoir sedimentation into closer agreement.

3.8. Watershed, Stream, Stream Corridor, and Within-Channel Variables as Predictors of ND_{Res}

We developed a series of prediction equations using stepwise regression relating the variables to ND_{Res} but limited the number of variables to five to minimize over-fitting the equations. The best models are shown in Table 16 (alternative models are provided in Supplemental Table S12). The best one-variable model used accounted for ~44% of the variability of ND_{Res} using $LNWS_K$. The equation indicates that as the overall watershed soil erosivity increased, ND_{Res} became less negative. Refs. [19,20] noted that RUSLE erosion estimates were >100% in some instances. Assuming the RUSLE overestimates soil erosion, the equation implies that the dominance of highly erosive soils in a watershed may compensate, to some degree, the RUSLE bias or "baseline" effect when trying to estimate reservoir sedimentation. However, the amount of overestimation is unknown for our watersheds. The one-variable model cannot account for well over one-half of

the variation of ND_{Res} , thereby limiting the usefulness of this model. The two-variable model accounted for ~72% (adjusted R^2) of the variability in ND_{RES} using $^{SHASH}ER$ and $FWA_ \%WA$. As ER increases (i.e., stream entrenchment decreases), underestimation of measured reservoir sedimentation increases. Less entrenched streams are better connected to their floodplains [31] providing an increased opportunity for the redeposition of sediment (from all sources), thereby impeding and delaying sediment delivery to the receiving reservoir. This, in combination with the assumed RUSLE overprediction of soil erosion, may account for the increased discrepancy between the GIS-based RUSLE estimates of reservoir sedimentation and observed data. The $FWA_ \%WA$ variable somewhat mitigates the effects of the ER variable because, as it increases, the ND_{Res} value becomes less negative. This may be due to probable increased generation of sediments by larger FWAs (i.e., larger wetted perimeter) as compared to those that are smaller. The three-variable model included ^{LN}BFD , $FWA_ \%WA$, and IC_K and accounted for ~82% of the variability in ND_{Res} . The role of $FWA_ \%WA$ is the same as that described for the two-variable model, and the role of IC_K is like that described for WS_K in the one-variable model; however, the relationship between IC_K and ND_{Res} is stronger than that of WS_K and ND_{Res} . As the BFD increases, the ND_{Res} becomes increasingly negative. Larger BFDs indicate that more stream bank area is exposed to erosive processes, thereby contributing more sediment to the receiving reservoirs and for which the RUSLE model cannot account [19]. The four-variable model accounts for ~95% of the variation in ND_{Res} and includes the previously discussed WS_K and ER variables as well as the log-normal versions of W_{v1} and $Cor_{slope \geq 21} : W_{v1}$. Regarding W_{v1} , it is noted that as the value of this variable increases so does the degree of underestimation of measured reservoir sedimentation. This variable may be related to an increasing probability of sediment contributions from gullies, stream channels, and stream banks as the watershed valley length increases. The $Cor_{slope \geq 21} : W_{v1}$ behaves similarly to W_{v1} , but is a better indicator of likely gully and stream bank sources of sediment within the 100 m corridor of the stream not accounted for by the RUSLE model. The five-variable model accounts for ~98% of the variability of ND_{Res} and includes one variable not discussed heretofore—the WA. From the regression model, it can be noted that as WA increases, the underestimation of measured sedimentation decreases. This variable is likely related to the SDRs used in the GIS-based RUSLE/SEDIMENTATION simulations of the respective watersheds. As noted earlier, the SDR is based on WA and has been formulated on the general observation that as WA increases, sediment delivery to the receiving reservoirs decreases.

Table 16. Root mean square error (RMSE), multiple coefficient of determination (R^2), and adjusted R^2 for the best 1- to 5-variable linear regression models. Non-normally distributed values were transformed using either a log-normal (LN) or sineh-arcsineh (SHASH) transformation and are indicated as a superscripted prefix to the affected variable. The regression equations and their p -values are also shown.

# Model Variables	Variables Used	RMSE (%)	R^2	Adjusted R^2	p -Value
1	$^{LN}WS_K$ $ND_{Res} = (117.3 \times ^{LN}WS_K) - 103.6$	11.7	0.436	---	0.0194
2	$^{SHASH}ER, FWA_ \%WA$ $ND_{Res} = (-31.0 \times ^{SHASH}ER) + (7.1 \times FWA_ \%WA) - 79.4$	7.8	0.775	0.724	0.0012
3	$^{LN}BFD, FWA_ \%WA, \%IC_K$ $ND_{Res} = (243.7 \times \%IC_K) + (7.0 \times FWA_ \%WA) - (30.7 \times ^{LN}BFD) - 145.7$	6.2	0.871	0.822	0.0006
4	$^{LN}W_K, ^{LN}W_{v1}, ^{LN}Cor_{slope \geq 21} : W_{v1}, ^{SHASH}ER$ $ND_{Res} = (62.5 \times ^{LN}W_K) - (64.8 \times ^{SHASH}ER) - (82.2 \times ^{LN}Cor_{slope \geq 21} : W_{v1}) - (46.2) - 8.8$	3.4	0.967	0.948	<0.0001
5	$^{LN}W_A, ^{LN}WS_K, ^{LN}W_{v1}, ^{LN}Cor_{slope \geq 21} : W_{v1}, ^{SHASH}ER$ $ND_{Res} = (41.1 \times ^{LN}W_A) + (86.5 \times ^{LN}W_K) - (107.7 \times ^{LN}W_{v1}) - (124.1 \times ^{LN}Cor_{slope \geq 21} : W_{v1}) - (91.1 \times ^{SHASH}ER)$	1.9	0.991	0.984	<0.0001

4. Conclusions

Three objectives guided this research study. Objective 1 sought to evaluate the impact of temporal variations of the RUSLE C-factor on the estimation of reservoir sedimentation. To this end, we used land cover maps to determine C-factors of five dates for 12 watersheds located in the Little Washita River Experimental Watershed. Evaluation of the GIS-based RUSLE simulations indicated that there were no statistical differences in the sedimentation estimates when all watersheds were pooled over all dates. Yet, there were large practical differences between some years. There were also no statistical differences in estimates of reservoir sedimentation within the Crop and Grass subdominant land cover groups; however, there were statistical differences between the 1985 and 1989 dates within the Tree/Shrub group. For reservoir sedimentation studies, it is advisable to run simulations for several different years to capture the impact of temporally variable C-factors to better account for variations in overland sediment contributions to reservoir sedimentation.

It has been noted that a primary weakness of RUSLE is its inability to account for sediments derived from gully, stream channel, and stream bank sources. In Objective 2 we conducted a first-order (regionally based) adjustment to compensate for these sources by reducing the measured reservoir sediment. This adjustment resulted in closer agreement between estimated and measured sedimentation for all 12 watersheds, but better agreement occurred for five watersheds where the difference between GIS-based RULSE estimated and measured sedimentation averaged $-6.0 \pm 11.8\%$. Although the agreement between estimated and measured reservoir sedimentation improved somewhat for the remaining seven watersheds, average underestimation was still large ($-65.1 \pm 9.3\%$). Thus, it is apparent that a regionally based adjustment will not likely be adequate to bring RUSLE-based estimated of reservoir sedimentation in line with measured data. It was also shown that unrealistic SDRs would be required to bring model simulations of reservoir sedimentation into agreement with measured data, under the conditions specified in this study.

Analyses of the linkage between watershed, stream, stream corridor, and within-channel variables (objective 3) showed strong relationships between selected geomorphic, pedologic, and topographic variables and the degree to which measured reservoir sedimentation was underpredicted using the GIS-based RUSLE model. The parameter values for the linear regression models developed in this study are not likely applicable to conditions vastly different from those presented herein. However, it is anticipated that the variables used in the regression equations may be sufficient to characterize the impact of these watershed, stream, and within-channel characteristics on reservoir sedimentation or to group watersheds into classes representing a probable difference between simulated and measured reservoir sedimentation. Such an approach could be used to prioritize reservoirs for evaluation of structure life and safety standards.

Supplementary Materials: The following supporting information can be downloaded at: <https://www.mdpi.com/article/10.3390/land12101913/s1>, Table S1: Sinuosity (Ssn) values and their interpretation; Table S2: Bank height ratio (BHR) values with accompanying stability assignment; Table S3: Bank height (BH) and Bank Angle (BA) values with accompanying category assignment; Table S4: Entrenchment ratio (ER) and Bank Full width:Bank Full Depth ratio (BFW:BFD) values with accompanying category assignment; Table S5: Year, satellite sensor, horizontal spatial resolution, and classification schemes used to develop land cover/C-factor data; Table S6: Mean, maximum, minimum, and standard deviation as decimal percents of watershed area in either Crop, Fallow, Grass, or Tree/Shrub; Table S7: Watershed basin relief (Wrlf), percentage of watershed having slopes $\geq 21^\circ$ (%Wslope \geq), watershed valley length (Wvl), stream thalweg length (Sthal), stream slope (Sslope), and stream sinuosity (Ssn) for each watershed; Table S8: Percentage of 100-m stream buffer area having slopes $\geq 21^\circ$ (%Corslope ≥ 21), ratio of %Corslope $\geq 21^\circ$ to Wvl (Corslope ≥ 21 :WVL), and percentage of buffer area with low, moderate, or high K-f actor soils (%CorLK, %CorMK, %CorHK) for each watershed; Table S9: Within-channel, stream segment weighted values of bank full depth (BFD), bank full width (BFW), ratio of BFW to BFD (BFW:BFD), entrenchment ratio (ER), bank angle (BA), bank height ratio (BHR), channel depth (CD), channel width (CW), ratio of CW to CD (CW:CD), channel cross-sectional area (CA), and horizontal stream surface area as a percentage of watershed

drainage area (FWA_%WA) for each watershed; Table S10: Within-channel, stream segment weighted values of weighted soil sand and silt fractions (ICS_a and ICS_i, respectively), percent of streambed and streambank soils that have low, moderate, or high K-factors (%IC_{LK}, %IC_{MK}, and %IC_{HK}), a weighted K-factor value ICK, and the plasticity index (ICPI) for each watershed; Table S11: Normalized difference of estimated reservoir sedimentation with first-order adjustment for stream channel, stream bank, and gully contributions of sediment (NDR_{es_adj}) from GIS-based RUSLE model simulations using the USDA [41] and Garbrecht [39] sediment delivery ratios (SDR) for each watershed (ID) in Group 2; Table S12: Root mean square error (RMSE), multiple coefficient of determination (R²), and adjusted R² for alternative linear regression models; Figures S1 through S12: GIS images of (a) slope (deg), (b) K-factor [(metric ton*ha*hr)/(ha*MJ*mm)], (c) RUSLE total annual soil loss for each patch (metric tons yr⁻¹), and (d) SEDIMENTATION net annual soil loss for each patch (metric tons yr⁻¹) for watersheds 11, 14, 20, 21, 22, 23, 24, 26, 31, 39, 41, and 42, respectively; Figures S13 through S24: C-factor images for watersheds 11, 1, 20, 21, 22, 23, 24, 26, 31, 39, 41, and 42, respectively. References [45–47] are cited in the supplementary materials.

Author Contributions: Experimental design: P.J.S. and D.N.M.; Methodology: P.J.S.; Formal analysis: P.J.S., D.N.M. and A.-M.F.; Writing—original draft: P.J.S.; Writing—revision and editing: P.J.S., A.-M.F. and D.N.M. All authors have read and agreed to the published version of the manuscript.

Funding: This research was supported by the USDA-ARS Office of National Programs (project number: 3070-13000-13-00D), the USDA-NRCS CEAP (Conservation Effects Assessment Project), and the USDA-LTAR (Long-Term Agroecosystem Research) network.

Data Availability Statement: Data sources for the publicly available data have been provided in the manuscript. Summary data presented in this study are available in the supplementary materials.

Acknowledgments: The authors would like to thank V. Hall for acquiring, downloading, and preprocessing the various GIS data sets required for this study.

Conflicts of Interest: The authors declare no conflict of interest for this study. Mention of trade names or commercial products in this publication is solely for the purpose of providing specific information and does not imply recommendation or endorsement by the U.S. Department of Agriculture. The USDA is an equal opportunity provider and employer.

Abbreviations

Acronym	Meaning
%Cor _{HK}	Percentage of the 100 m stream corridor area having high K-factor soils
%Cor _{LK}	Percentage of the 100 m stream corridor area having low K-factor soils
%Cor _{MK}	Percentage of the 100 m stream corridor area having moderate K-factor soils
%Cor _{slope ≥ 21}	Percentage of the 100 m stream corridor area having slopes ≥ 21°
%IC _{HK}	Weighted percentage of high K-factor soils composing the stream bank and channel
%IC _{LK}	Weighted percentage of low K-factor soils composing the stream bank and channel
%IC _{MK}	Weighted percentage of moderate K-factor soils composing the stream bank and channel
%IC _{WK}	Weighted average K-factor of the stream bank and stream channel soils
%W _{slope > 21}	Percentage of the WA having slopes ≥ 21°
ANOVA	Analysis of Variance
BA	Bank angle (deg)
BFD	Bank full depth (m)
BFW	Bank full width (m)
BFW:BFD	Ratio of BFW to BFD
BH	Bank height (m)
BHR	Bank height ratio
BSTEM	Bank Stability and Toe Erosion Model
CA	Stream channel area (m ²)
CD	Stream channel depth (m)
CW	Stream channel width (m)
CW:CD	Ratio of CW to CD
Cor _{slope ≥ 21}	Actual area of the 100 m stream corridor having slopes ≥ 21° (m ²)
Cor _{slope ≥ 21} :W _{v1}	Area within the 100 m stream corridor having slopes ≥ 21° per m of W _{v1} (m ² m ⁻¹)

DEM	Digital elevation model
ER	Entrenchment ratio
EUROSEM	European Soil Erosion Model
FP	Flood plain
FWA	Flood way area
GIS	Geographical information system
IC	Within-channel
IC _{PI}	Weighted average plasticity index of the stream bank and stream channel soils
IC _{Sa}	Weighted average sand fraction of the stream bank and stream channel soils
IC _{Si}	Weighted average silt fraction of the stream bank and stream channel soils
LWREW	Little Washita River Experimental Watershed
ND _{Res}	Normalized difference between estimated and measured sedimentation
ND _{Res_adj}	ND _{Res} adjusted to account for stream channel/bank sediment contributions
ND _{ResT}	Johnson Su transformation of ND _{Res}
RMSE	Root mean square error
RUSLE	Revised Universal Soil Loss Equation
RUSLE2	RUSLE version 2
SDR	Sediment delivery ratio
SE	Total soil erosion
SY	Sediment yield
S _{slope}	Stream slope (m m ⁻¹)
S _{sn}	Stream sinuosity
S _{thal}	Stream thalweg length (m)
USLE	Universal soil loss equation
USDA-NRCS	United States Department of Agriculture-Natural Resources Conservation Service
WEPP	Water Erosion Prediction Project
WRB	Washita River Basin
W _A	Watershed drainage area (km ²)
W _{HK}	Percentage of watershed drainage area in high K-factor soils
W _{LK}	Percentage of watershed drainage area in low K-factor soils
W _K	Area-weighted watershed K-factor
W _{MK}	Percentage of watershed drainage area in moderate K-factor soils
W _{rlf}	Watershed relief (m)
W _{vl}	Watershed valley length (m)

References

- Moriasi, D.N.; Steiner, J.L.; Duke, S.E.; Starks, P.J.; Verser, A.J. Reservoir sedimentation rates in the Little Washita River experimental watershed: Measurement and controlling factors. *J. Amer. Water Resour. Assoc.* **2018**, *54*, 1011–1023. [[CrossRef](#)]
- Hanson, G.J.; Caldwell, L.; Lobrecht, M.; McCook, D.; Hunt, S.L.; Temple, D. A look at the engineering challenges of the USDA Small Watershed Program. *Centennial Edition Trans. ASABE* **2007**, *50*, 1677–1682. [[CrossRef](#)]
- Hunt, S.L.; Hanson, G.L.; Temple, D.M.; Caldwell, L. The importance of the USDA Small Watershed Program to the rural United States. *Water Resour. IMPACT* **2011**, *13*, 9–11.
- Allen, P.B.; Naney, J.W. *Hydrology of the Little Washita River Watershed, Oklahoma*; United States Department of Agriculture, Agricultural Research Service: Washington, DC, USA, 1991; ARS-90.
- Bennett, S.J.; Dunbar, J.A.; Rhoton, F.E.; Allen, P.M.; Bigham, J.M.; Davidson, G.R.; Wren, D.G. Assessing sedimentation issues within aging flood-control reservoirs. *Rev. Engin. Geol.* **2013**, *21*, 25–44.
- Ketchum, A.J.; Mathew, P.E.; Lyons, P.E.; Evans, R. *Reservoir Sediment Impacts on the Rehabilitation of NRCS-Assisted Flood Control Dams in Virginia*; ASABE Paper No. 1900198; American Society of Agricultural and Biological Engineers: St. Joseph, MI, USA, 2019; 3p.
- Zhang, X.C.J.; Zhang, G.H.; Wei, X.; Guan, Y.H. Evaluation of cesium-137 conversion models and parameter sensitivity for erosion estimation. *J. Environ. Qual.* **2015**, *44*, 789–802. [[CrossRef](#)]
- The Small Watershed Rehabilitation Amendments of 2000. Available online: <https://www.congress.gov/bill/106th-congress/house-bill/728> (accessed on 7 August 2023).
- Laflen, J.M.; Elliot, W.J.; Flanagan, D.C.; Meyer, C.R.; Nearing, M.A. WEPP-predicting water erosion using a process-based model. *J. Soil Water Conserv.* **1997**, *52*, 96–102.
- Morgan, R.P.C.; Quinton, J.N.; Smith, R.E.; Govers, G.; Poesen, J.W.A.; Auerswald, K.; Chisci, G.; Torri, D.; Styczen, M.E. The European Soil Erosion Model (EUROSEM): A dynamic approach for predicting sediment transport from fields and small catchments. *Earth Surf. Proc. Landforms J. Brit. Geomorph. Group* **1998**, *23*, 527–544. [[CrossRef](#)]

11. Kinnell, P.I. Sediment delivery ratios: A misaligned approach to determining sediment delivery from hillslopes. *Hydrolog. Proc.* **2004**, *18*, 3191–3194. [CrossRef]
12. Renard, K.G.; Foster, G.R.; Weesies, G.A.; McCool, D.K.; Yoder, D.C. *Predicting Soil Erosion by Water: A Guide to Conservation Planning with the Revised Soil Loss Equation (RUSLE)*; Agriculture Handbook No. 703; United States Department of Agriculture: Washington, DC, USA, 1997; 404p.
13. Wischmeier, W.H.; Smith, D.D. *Predicting Rainfall Erosion Losses—A Guide to Conservation Planning*; U.S. Department of Agriculture, Handbook No. 537; United States Department of Agriculture: Washington, DC, USA, 1978.
14. Shi, Z.H.; Cai, C.F.; Ding, S.W.; Wang, T.W.; Chow, T.L. Soil conservation planning at the small watershed level using RUSLE with GIS: A case study in the Three Gorges area of China. *Catena* **2004**, *55*, 33–48. [CrossRef]
15. Chen, H.; El Garouani, A.; Lewis, L.A. Modelling soil erosion and deposition within a Mediterranean mountainous environment utilizing remote sensing and GIS—Wadi Tlata, Morocco. *Geograph. Helvet.* **2008**, *63*, 36–47. [CrossRef]
16. Anees, M.T.; Abdullah, K.; Nawawi, M.N.M.; Norulaini, N.A.N.; Syakir, M.I.; Omar, A.K.M. Soil erosion analysis by RUSLE and sediment yield models using remote sensing and GIS in Kelantan state, Peninsular Malaysia. *Soil Res.* **2018**, *56*, 356–372. [CrossRef]
17. Kumar, A.; Devi, M.; Deshmukh, B. Integrated Remote Sensing and Geographic Information System Based RUSLE Modelling for Estimation of Soil Loss in Western Himalaya, India. *Water Resour. Manag.* **2014**, *28*, 3307–3317. [CrossRef]
18. Kouli, M.; Soupios, P.; Vallianatos, F. Soil erosion prediction using the Revised Universal Soil Loss Equation (RUSLE) in a GIS framework, Chania, Northwestern Crete, Greece. *Environ. Geol.* **2009**, *57*, 483–497. [CrossRef]
19. Boomer, K.B.; Weller, D.E.; Jordan, T.E. Empirical models based on the Universal Soil Loss Equation fail to predict sediment discharges from Chesapeake catchments. *J. Environ. Qual.* **2008**, *37*, 79–89. [CrossRef]
20. Moges, M.M.; Abay, D.; Engidayehu, H. Investigating reservoir sedimentation and its implications to watershed sediment yield: The case of two small dams in data-scarce upper Blue Nile basin, Ethiopia. *Lakes and Reser.* **2018**, *23*, 217–229. [CrossRef]
21. Kaffas, K.; Pisinaras, V.; Al Sayah, M.J.; Santopietro, S.; Righetti, M. A USLE-based model with modified LS-factor combined with sediment delivery module for Alpine basins. *Catena* **2021**, *207*, 105655. [CrossRef]
22. Bufalini, M.; Materazzi, M.; Martinello, C.; Rotigliano, E.; Pambianchi, G.; Tromboni, M.; Paniccia, M. Soil erosion and deposition rate inside an artificial reservoir in central Italy: Bathymetry versus RUSLE and morphometry. *Land* **2022**, *11*, 1924. [CrossRef]
23. Trimble, S.W. Contribution of stream channel erosion to sediment yield from an urbanizing watershed. *Science* **1997**, *278*, 1442–1444. [CrossRef]
24. Prosser, I.P.; Rutherford, I.D.; Olley, J.M.; Young, W.J.; Wallbrink, P.J.; Moran, C.J. Large-scale patterns of erosion and sediment transport in river networks, with examples from Australia. *Mar. Freshw. Res.* **2001**, *52*, 81–99. [CrossRef]
25. Basher, L.; Douglas, G.; Elliott, S.; Hughes, A.; Jones, H.; McIvor, I.; Page, M.; Rosser, B.; Tait, A. Impacts of Climate Change on Erosion and Erosion Control Methods—A Critical Review. Final Report MPI Technical Paper No: 2012/45, 2012. Available online: <https://www.mpi.govt.nz/document-vault/4074> (accessed on 8 March 2023).
26. Simon, A.; Rinaldi, M. Disturbance, stream incision, and channel evolution: The roles of excess transport capacity and boundary materials in controlling channel response. *Geomorphology* **2006**, *79*, 361–383. [CrossRef]
27. Wilson, C.G.; Kuhnle, R.A.; Bosch, D.D.; Steiner, J.L.; Starks, P.J.; Tomer, M.D.; Wilson, G.V. Quantifying relative contributions from sediment sources in Conservation Effects Assessment Project watersheds. *J. Soil Water Conser.* **2008**, *63*, 523–532. [CrossRef]
28. Simon, A.; Klimetz, L. Relative magnitudes and sources of sediment in benchmark watersheds of the Conservation Effects Assessment Project. *J. Soil Water Conser.* **2008**, *63*, 504–522. [CrossRef]
29. Benavidez, R.; Jackson, B.; Maxell, D.; Norton, K. A review of the (Revised) Universal Soil Loss Equation ((R)USLE): With a view to increasing its global applicability and improving soil loss estimates. *Hydrol. Earth Syst. Sci.* **2018**, *22*, 6059–6086. [CrossRef]
30. Oklahoma Climatological Survey. Available online: http://climate.ok.gov/index.php/climate/climate_normals_by_county/local_data (accessed on 7 August 2023).
31. Rosgen, D.L. A classification of natural rivers. *Catena* **1994**, *22*, 169–199. [CrossRef]
32. United States Department of Agriculture. *Site Assessment and Investigation. Part 654 Stream Restoration Design, Chapter 3, National Engineering Handbook*; USDA-Natural Resources Conservation Service: Washington, DC, USA, 2007. Available online: <https://directives.sc.egov.usda.gov/viewerFS.aspx?hid=21433> (accessed on 31 March 2023).
33. United States Department of Agriculture-Agricultural Research Service, Watershed Physical Processes Research: Oxford, MS. Available online: <https://www.ars.usda.gov/Research/docs.htm?docid=5044> (accessed on 30 March 2023).
34. Rosgen, D.L. A practical method of computing streambank erosion rate. In Proceedings of the Seventh Interagency Sedimentation Conference, Reno, NV, USA, 25–29 March 2001; Volume 2, pp. 9–15.
35. United States Department of Agriculture-Natural Resources Conservation Service. Web Soil Survey. Available online: <https://websoilsurvey.sc.egov.usda.gov/app/> (accessed on 22 September 2023).
36. United States Department of Agriculture-Natural Resources Research Service. Geospatial Data Gateway. Available online: <https://gdg.sc.egov.usda.gov/> (accessed on 22 September 2023).
37. Starks, P.J.; Steiner, J.L.; Stern, A.J. Upper Washita River experimental watersheds: Land cover data sets (1974–2007) for two southwestern Oklahoma agricultural watersheds. *J. Environ. Qual.* **2014**, *43*, 310–318. [CrossRef]
38. United States Department of Agriculture-Natural Resources Conservation Service. Available online: https://efotg.sc.egov.usda.gov/references/Agency/OK/RUSLE_Chap4_C_Factors.pdf (accessed on 23 March 2023).

39. Garbrecht, J.D. Effects of climate variations and soil conservation on sedimentation of a west-central Oklahoma reservoir. *J. Hydrol. Eng.* **2011**, *16*, 899–906. [[CrossRef](#)]
40. Maner, S.B. Factors affecting sediment delivery ratios in the Red Hills physiographic area. *Trans. Amer. Geophys. Union* **1958**, *39*, 669–675. [[CrossRef](#)]
41. United States Department of Agriculture. Sediment sources, yields, and delivery ratios. In *National Engineering Handbook*; Section 3; Sedimentation; United States Department of Agriculture: Washington, DC, USA, 1972.
42. Boyce, R.C. Sediment routing with sediment delivery ratios. In *Present and Prospective Technology for Predicting Sediment Yields and Sources*; Publication ARS-S-40; United States Department of Agriculture: Washington, DC, USA, 1975; pp. 61–65.
43. Vanoni, V.A. *Sedimentation Engineering*; American Society of Civil Engineers: Reston, VA, USA, 2006.
44. Johnson, N.L. Systems of frequency curves generated by methods of translation. *Biometrika* **1949**, *36*, 149–176. [[CrossRef](#)]
45. Schumm, A.A. Patterns of alluvial rivers. *Ann. Rev. Earth and Planet. Sci.* **1985**, *13*, 5–27. [[CrossRef](#)]
46. New Mexico State University. Available online: https://jornada.nmsu.edu/files/geomorp_terms.pdf (accessed on 24 April 2023).
47. United States Department of Agriculture. Rosgen Stream Classification Technique Supplemental Materials. Technical Supplement 3, Part 654, National Engineering Handbook. Available online: <https://directives.sc.egov.usda.gov/rollupviewer.aspx?hid=17092> (accessed on 25 April 2023).

Disclaimer/Publisher’s Note: The statements, opinions and data contained in all publications are solely those of the individual author(s) and contributor(s) and not of MDPI and/or the editor(s). MDPI and/or the editor(s) disclaim responsibility for any injury to people or property resulting from any ideas, methods, instructions or products referred to in the content.